Bioorganic & Medicinal Chemistry 17 (2009) 7113–7125

Contents lists available at ScienceDirect

Bioorganic & Medicinal Chemistry

journal homepage: www.elsevier.com/locate/bmc

Synthesis and evaluation of novel α-heteroaryl-phenylpropanoic acid derivatives as PPARα/γ dual agonists

Agustin Casimiro-Garcia [a,*], Christopher F. Bigge [a], Jo Ann Davis [b], Teresa Padalino [c], James Pulaski [b], Jeffrey F. Ohren [a], Patrick McConnell [a], Christopher D. Kane [d], Lori J. Royer [d], Kimberly A. Stevens [d], Bruce Auerbach [b], Wendy Collard [e], Christine McGregor [b], Kun Song [d]

[a] Department of Chemistry, Pfizer Global Research and Development, Michigan Laboratories, 2800 Plymouth Rd, Ann Arbor, MI 48105, USA
[b] Department of Cardiovascular Pharmacology, Pfizer Global Research and Development, Michigan Laboratories, 2800 Plymouth Rd, Ann Arbor, MI 48105, USA
[c] Department of Discovery Biomarkers, Pfizer Global Research and Development, Michigan Laboratories, 2800 Plymouth Rd, Ann Arbor, MI 48105, USA
[d] Department of Cardiovascular, Metabolic and Endocrine Diseases, Pfizer Global Research and Development, Groton Laboratories, Eastern Point Road, Groton, CT 06340, USA
[e] Department of Pharmacokinetics, Dynamics, and Metabolism, Pfizer Global Research and Development, Michigan Laboratories, 2800 Plymouth Rd, Ann Arbor, MI 48105, USA

ARTICLE INFO

Article history:
Received 16 July 2009
Revised 31 August 2009
Accepted 2 September 2009
Available online 6 September 2009

Keywords:
PPAR
PPARα/γ dual agonist
Type 2 diabetes
Phenylpropanoic acid

ABSTRACT

The synthesis of a new series of phenylpropanoic acid derivatives incorporating an heteroaryl group at the α-position and their evaluation for binding and activation of PPARα and PPARγ are presented in this report. Among the new compounds, (*S*)-3-{4-[3-(5-methyl-2-phenyl-oxazol-4-yl)-propyl]-phenyl}-2-1,2,3-triazol-2-yl-propionic acid (**17j**), was identified as a potent human PPARα/γ dual agonist (EC_{50} = 0.013 and 0.061 μM, respectively) with demonstrated oral bioavailability in rat and dog. **17j** was shown to decrease insulin levels, plasma glucose, and triglycerides in the ZDF female rat model. In the human apolipoprotein A-1/CETP transgenic mouse model **17j** produced increases in hApoA1 and HDL-C and decreases in plasma triglycerides. The increased potency for binding and activation of both PPAR subtypes observed with **17j** when compared to previous analogs in this series was explained based on results derived from crystallographic and modeling studies.

1. Introduction

The peroxisome-proliferator activated receptors (PPARs) are ligand-activated transcription factors that constitute a subfamily of nuclear receptors.[1,2] PPARs have a central role in regulating the storage and catabolism of lipids in both humans and animals. PPARα is a modulator of fatty acid catabolism that regulates the expression of genes involved in lipid and lipoprotein metabolism.[3] PPARα activation mediates the lipid-lowering activity of the fibrates, a class of agents used clinically to treat dyslipidemias. This class of agents, which includes the marketed drugs gemfibrozil (**1**) and fenofibrate (**2**), shown in Figure 1, can produce a significant reduction of serum triglycerides and a modest increase of high-density lipoprotein (HDL) cholesterol levels. In addition, activation of PPARα has been reported to produce insulin sensitizing effects and to improve glucose tolerance in type 2 diabetic patients.[4–6]

PPARγ is a critical modulator of adipocyte differentiation and function.[1,2] PPARγ activation also leads to modulation of genes involved in lipid metabolism and hormones that affect whole body energy metabolism. PPARγ was identified as the primary molecular target responsible for the glucose lowering activity of the thiazolidinedione (TZD) class of antihyperglycemic agents.[7] The two TZDs currently on the market, rosiglitazone (**3**) and pioglitazone (**4**) (structures presented in Fig. 1), have been shown to increase insulin sensitivity in target tissues and reduce glucose, triglyceride, and insulin levels in animal models of type 2 diabetes and in humans. Unfortunately, along with their beneficial effects, they also produce undesirable side effects including weight gain and edema.[8] The desire to positively impact both dyslipidemic and diabetic endpoints through simultaneous activation of both PPARα and PPARγ has spurred a search for safe PPARα/γ dual agonists.[9–12]

In recent years, a large number of PPARα/γ dual agonists have been characterized in vitro and in different animal models of type 2 diabetes and dyslipidemia. In addition, several of these agents reached clinical evaluation, including farglitazar (**5**),[13] ragaglitazar (**6**),[14] tesaglitazar (**7**),[15] KRP-297/MK-767 (**8**),[16] and muraglitzar (**9**).[17] Although these compounds had to be withdrawn from development at advanced stages due to different limitations and side effects including cardiovascular events and carcinogenicity in rodents, the clinical data generated with these compounds support the utility of PPARα/γ dual agonists for improving the pathological lipid profiles and hyperglycemia observed in type 2 diabetes and the metabolic syndrome.[18] Results from clinical studies with dual agonists **5**–**9** that display significantly higher PPARγ affinity than PPARα affinity have shown a profile in which the PPARγ-mediated

* Corresponding author. Tel.: +1 860 686 9155; fax: +1 860 715 4483.
E-mail address: agustin.casimiro-garcia@pfizer.com (A. Casimiro-Garcia).

0968-0896/$ - see front matter © 2009 Elsevier Ltd. All rights reserved.
doi:10.1016/j.bmc.2009.09.001

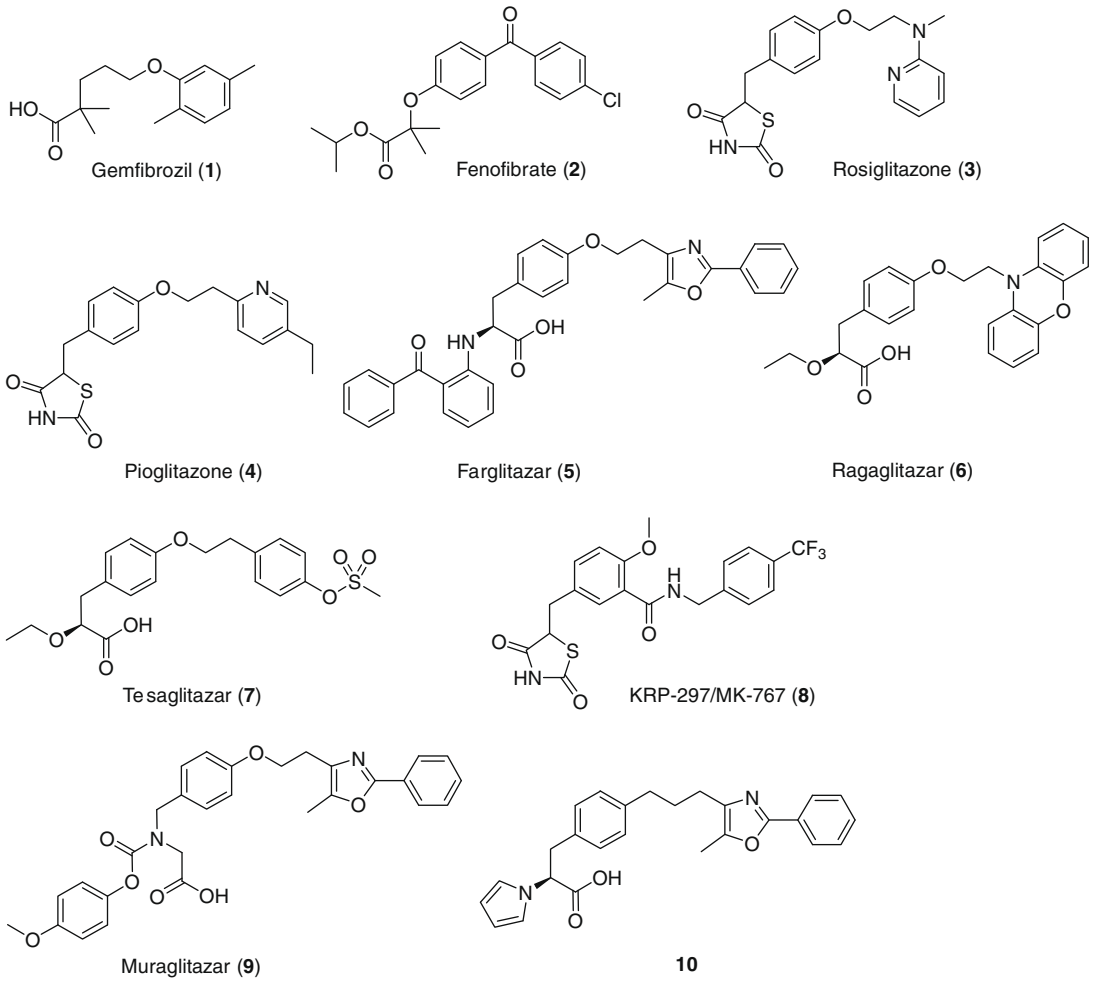

Figure 1. Chemical structures of marketed fibrates and glitazones and selected PPARα/γ dual agonists.

undesired effects were still observed.[9] Therefore, we hypothesized that a better profile might be obtained with dual agonists possessing a more balanced activity pattern. Based on this, further investigation of new PPARα/γ dual agonists with novel profiles remains an important area of research.

Our group recently reported a new series of phenylpropanoic acid derivatives that was designed with two objectives in mind:[19] (a) modulation of activity at each PPAR receptor subtype, and (b) identification of novel chemical space within the phenylpropanoic acid-based class of PPARα/γ dual agonists.[9a,10,12] Our strategies to accomplish these goals were to pursue modifications in the composition and nature of the linker that joins the central phenyl ring and the lipophilic tail (Fig. 2) and to change the group at the α-position of the phenylpropanoic acid scaffold. In these compounds, the commonly encountered ether linker was replaced with acetylene-, ethylene-, propyl-, or nitrogen-derived linkers. Results from this study indicated that changes in the linker region of the molecule led to noticeable effects in the binding and activation of PPARα and PPARγ. Of particular interest was the observation that these modifications caused a reduction in the potency for binding and activation of PPARγ, while maintaining similar activity on PPARα, when compared with compounds containing the ether linker. It was hypothesized that this may provide an opportunity to obtain compounds with either a balanced profile or greater selectivity for PPARα. It was also demonstrated that compounds with a propyl linker had in vitro profiles in line with our objectives, including increased binding and activation of PPARα and a more balanced γ:α

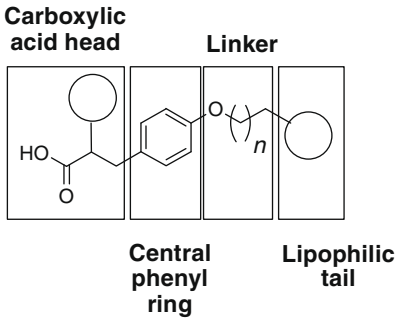

Figure 2. Schematic representation of the structure of phenylpropanoic acid based dual PPARα/γ agonists.

ratio based on EC_{50} values derived from transactivation assays ($CH_2CH_2CH_2$: 4:1; $NHCH_2CH_2$: 5:1; $C{\equiv}CCH_2$: 6:1; OCH_2CH_2: 26:1; $CH{=}CHCH_2$: 27:1), than compounds with other moieties. Among them, **10** demonstrated plasma glucose lowering activity comparable to rosiglitazone, but superior effects on the reduction of triglycerides, insulin, and free fatty acids in the Zucker diabetic fatty (ZDF) male rat, an obese rodent model of type 2 diabetes. The interactions of **10** with the ligand binding domain (LBD) of human PPARγ and PPARα were characterized by crystallography and modeling studies, respectively. They showed, as illustrated in Figure 3 for PPARγ, that **10** binds to the activated PPARγ receptor with

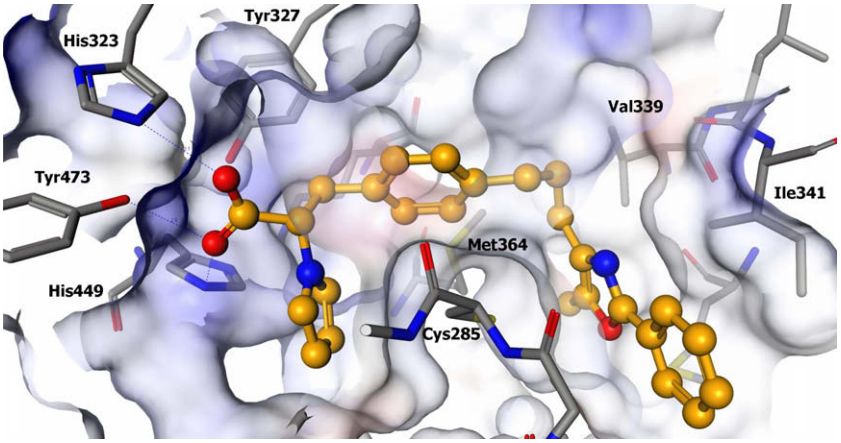

Figure 3. Three-dimensional surface representation of **10** (gold) bound in the ligand binding pocket of human PPARγ (gray). The figure shows the carboxylate head group of **10** forming a hydrogen bond network involving the 'charge clamp' residues His323 and Tyr327 from helix 6, His449 from helix 11, and Tyr473 from the activation helix 12.[19]

its carboxylate head group forming a hydrogen bond network involving the 'charge clamp' residues His323 and Tyr327 from helix 6, His449 from helix 11, and Tyr473 from the activation helix 12.[20]

As discussed above, our second strategy to modulate activity at each PPAR receptor subtype and identify novel chemical space was to modify the group at the α-position of the phenylpropanoic acid scaffold. However, the scope of our investigation in this region of the scaffold in the previous report was limited and it only included pyrrole, phenyl, biphenyl and 3-pyridinyl groups, with pyrrole being significantly better in terms of potency than the other moieties. Further studies with crystallography and modeling results suggested a variety of five-membered ring heterocycles at the α-position of the scaffold as suitable replacements for the pyrrole of **10**. We decided to embark upon a new investigation to identify novel PPARα/γ dual agonists with: (a) PPARγ potency similar to that of **10**, but with increased PPARα potency in binding and activation assays, and thus looking for a more balanced agonist; (b) pharmacokinetic properties suitable for oral administration. The modulation of activity at each PPAR subtype was planned to be achieved with two design elements: incorporation of the propyl linker and a five-membered ring heterocycle at the α-position of the scaffold. A description of the results of this investigation and the discovery of **17j**, a potent human PPARα/γ dual agonist, are presented in this report.

2. Chemistry

The synthesis of the new compounds was performed using an efficient and general method that utilizes the B-alkyl Suzuki–Miyaura cross-coupling between oxazole derivative **13** and bromides **15** (Scheme 1).[21,22] Oxazole **13** was prepared in two steps from benzamidoacetone (**11**). Deprotonation of **11** with lithium bis(trimethylsilyl)amide at low temperature,[23] followed by treatment of the resulting enolate with allyl bromide, provided the C-alkylated product **12**. Cyclization of this intermediate using trifluoroacetic acid/trifluoroacetic anhydride provided **13**. The aryl bromides utilized for the synthesis of the new compounds were obtained by first performing the deprotonation of 2-substituted acetates **14** with lithium bis(trimethylsilyl)amide or lithium diisopropylamide at low temperature, followed by alkylation of the resulting enolate with 4-bromobenzyl bromide to afford bromides **15**. Hydroboration of alkene **13** with a solution of 9-BBN in THF for 20 h at room temperature provided the B-alkyl-9-borabicyclo[3.3.1]nonane intermediate, which was then cross-coupled with bromides **15** under the conditions reported by Ohba and co-workers,[24] that consist

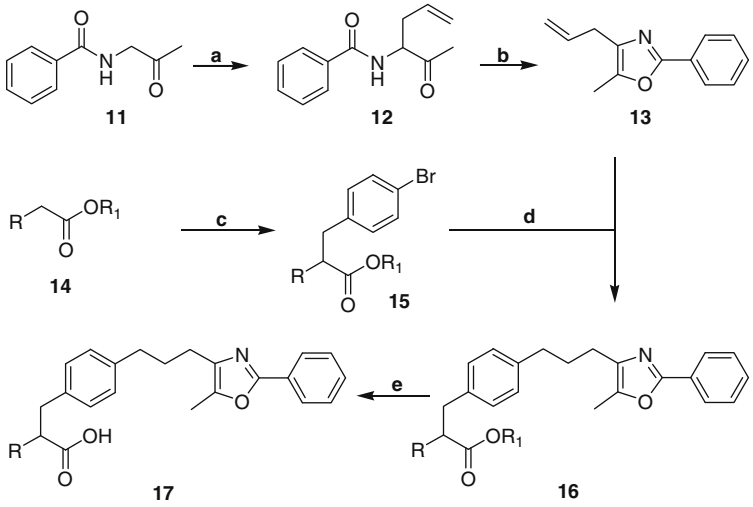

Scheme 1. Synthesis of new PPARα/γ dual agonists. Reagents and conditions: (a) (i) LHMDS, THF, −78 °C; (ii) allyl bromide, THF, −78 °C, 78%; (b) TFA, TFAA, 35–40 °C, 95%; (c) (i) LHMDS, THF, −40 °C, (ii) 4-bromobenzyl bromide, THF, −40 °C to rt; (d) (i) **13**, 9-BBN, THF, rt; (ii) **15**, $PdCl_2(dppf)$, Cs_2CO_3, Ph_3As, DMF–H_2O, rt; (e) LiOH, THF–H_2O.

in a mixture of $PdCl_2$(dppf) (10 mol %), triphenyl arsine (10 mol %) and cesium carbonate (1.8 equiv) in DMF–water at room temperature. In this manner, esters **16** (R_1 = methyl or ethyl) were obtained and were subsequently hydrolyzed utilizing lithium hydroxide in THF/water mixture to provide propanoic acid derivatives **17**. In some instances, pure enantiomers of specific compounds were required and the separation was achieved using chiral chromatography with a Chiralcel AD column. The assignment of the stereochemistry for these compounds was based on their biological activity and the well precedented higher binding affinity and potency to PPARγ of the *S*-enantiomer among pairs of enantiomers of TZDs, phenylpropanoic acid derivatives, and other PPARγ agonists including the series of compounds previously described by our group.[13,19,25–27]

3. Results and discussion

The new compounds were evaluated for their PPAR α and γ agonist activity in both cell-based and biochemical assays. The PPAR-GAL4 chimeric transactivation assays were performed in HepG2 cells and the results are expressed as EC_{50} values, defined as the concentration of test compound that produces 50% of maximal reporter activity. Additionally, selected compounds were also evaluated for their affinity for PPARα and PPARγ using scintillation proximity assays (SPA) and the results are reported as IC_{50} values for displacement of radiolabeled reference compound. The results of these assays are summarized in Table 1.

As stated earlier, further studies with crystallography and modeling results suggested that a variety of five-membered ring heterocycles at the α-position of the scaffold might provide suitable replacements for the pyrrole of **10**. Therefore, a number of compounds were synthesized. Initially, heterocyclic rings attached to the phenylpropanoic acid scaffold through a non-nitrogen link were evaluated. Comparison of **10** (α, EC_{50} = 0.623 μM; γ, EC_{50} = 0.140 μM) with **17a** (α, EC_{50} = 0.685 μM; γ, EC_{50} = 0.399 μM) showed that introduction of a more lipophilic heterocycle, a thiophen-3-yl group was well tolerated with limited impact on the potency for both PPAR subtypes, as determined from transactivation assays. It is interesting to point out that **17l** with a phenyl group, usually considered as bioisostere of thiophene, was found to be significantly less potent than **10** for both PPAR subtypes in our previous study.[19] This seems to suggest a preference for a smaller substituent at this position. Incorporation of the polar isoxazolyl group led to a decrease in potency as observed with **17b** and **17c** which incorporate an isoxazol-3-yl, or isoxazol-5-yl moiety, respectively, as the α-substituent. Both of these compounds exhibited greater than 10-fold reduction in activation for PPARα and γ, as determined from their EC_{50} values. In both compounds, additional steric bulk may have contributed to the drop in potency due to the presence of a methyl group attached to the heterocycle. We decided to evaluate other unsubstituted five-membered ring heterocycles attached to the phenylpropanoic scaffold through a nitrogen link. Introduction of pyrazole at the α-position of the scaffold led to **17d**. In transactivation assays, **17d** showed diminished potency for both PPAR subtypes, with larger decrease on PPARα (>4-fold), when compared to **10**. In order to investigate the activity of the active enantiomer of **17d**, this compound was subjected to resolution via chiral chromatography under the conditions mentioned above to provide **17e** and **17f**. The significantly higher potency of **17e** over **17f** in both binding (PPARγ: >200-fold) and activation (PPARα: >20-fold; PPARγ: >300-fold) assays led to the assignment of **17e** as the *S*-enantiomer. From a comparison between **10** and **17e** (α, EC_{50} = 0.874 μM; γ, EC_{50} = 0.065 μM), it was observed that in the *S*-enantiomer series incorporation of pyrazole as the α-substituent led to a two-fold increase in PPARγ potency without altering PPARα activity and agonist efficacy (**17e**: α: 65%; γ: 91%; **10**: α: 52%; γ: 94%), as assessed from transactivation assays. Unfortunately, this also showed that pyrazole in **17e** led to higher selectivity for PPARγ than for PPARα (γ:α ratio 13:1).

Incorporation of triazole at the α-position of the scaffold led to analogs derived from either 1,2,3-triazole or 1,2,4-triazole and this set of compounds led to particularly interesting results. Incorporation of a 1,2,4-triazol-1-yl ring in **17g**, or a 1,2,3-triazol-1-yl group in **17h**, was found to eliminate the binding and agonist activity for both PPAR subtypes. A completely opposite effect was observed when a 1,2,3-triazole ring derivatized at *N*-2 was incorporated in **17i**. This compound was significantly more potent than **10** in both binding and transactivation assays. Specifically, **17i** exhibited a 38-fold and 40-fold increase in binding potency for PPARα and PPARγ (IC_{50} = 0.024 μM and IC_{50} = 0.005 μM, respectively), when compared to **10** (α: IC_{50} = 0.912 μM; γ: IC_{50} = 0.185 μM). In transactivation assays, **17i** also exhibited increased potency, predominantly for PPARγ (**17i**, EC_{50} = 0.015 μM; **10**, EC_{50} = 0.140 μM). With the remarkable profile obtained with this compound, the separation

Table 1
In vitro PPAR binding and transactivation activity of new propanoic acid derivatives

Compd	R	Stereo[c]	TA EC_{50}[a] (μM)					Binding IC_{50}[b] (μM)	
			h-PPARγ (%max)[d]		h-PPARα (%max)[e]		γ:α Ratio	h-PPARγ	h-PPARα
Rosi (**3**)			0.223	(84)	>12	(23)	>54:1	0.274	21%[f]
10	Pyrrole	*S*	0.140	(94)	0.623	(52)	4:1	0.185	0.912
17a	Thiophene-3-yl	*rac*	0.399	(82)	0.685	(59)	2:1	1.6	0.676
17b	5-Methyl-isoxazol-3-yl	*rac*	1.9	(42)	5.7	(49)	3:1	14	NT
17c	3-Methyl-isoxazol-5-yl	*rac*	3.8	(56)	8.5	(48)	2:1	1.6	NT
17d	Pyrazol-1-yl	*rac*	0.228	(80)	2.6	(70)	11:1	0.327	0.877
17e	Pyrazol-1-yl	*S*	0.065	(91)	0.874	(65)	13:1	0.145	0.899
17f	Pyrazol-1-yl	*R*	>20	(NA)	>20	(NA)	1:1	33	NT
17g	1,2,4-Triazol-1-yl	*rac*	>30	(NA)	>100	(NA)	3:1	18	NT
17h	1,2,3-Triazol-1-yl	*rac*	>30	(NA)	>100	(NA)	3:1	14	NT
17i	1,2,3-Triazol-2-yl	*rac*	0.015	(88)	0.182	(64)	12:1	0.005	0.024
17j	1,2,3-Triazol-2-yl	*S*	0.013	(103)	0.061	(90)	5:1	0.003	0.034
17k	1,2,3-Triazol-2-yl	*R*	>20	(NA)	>20	(NA)	1:1	>70	>3.30
17l[g]	Phenyl	*rac*	3.9	(57)	5	(28)	1:1	4	>3.30

[a] TA (transactivation assay). Mean value of two determinations.
[b] Mean value of three determinations using scintillation proximity assay (SPA).
[c] Stereochemistry of the chiral center.
[d] The maximum efficacy of PPARγ activation of darglitazone was defined as 100%.
[e] The maximum efficacy of PPARα activation of GW9578 was defined as 100%.
[f] Inhibition at 10 μM.
[g] Values for **17l** taken from Ref. 19. NT = not tested. NA = no activation up to the concentration shown.

of enantiomers of **17i** was then pursued using the chiral chromatography conditions referred to previously. From this resolution, **17j** and **17k** were obtained and evaluated. The markedly different profile of these compounds enabled the identification of **17j** as the active enantiomer with the assumed *S*-configuration. Later X-ray crystallography studies of the complex of **17j** bound to the human PPAR-ligand binding domain determined to 2.30 Å resolution (see Section 3.1.) further supported the *S*-configuration assignment. In binding assays, **17j** showed a 26-fold and 61-fold increase in potency for PPARα and PPARγ (IC_{50} = 0.034 μM and IC_{50} = 0.003 μM, respectively), when compared to **10**. Also, **17j** exhibited an approximately 10-fold increase in potency for both PPAR subtypes in transactivation assays, while it retained similar agonist efficacy for PPARγ, but higher agonist efficacy for the α subtype (α, EC_{50} = 0.061 μM, %max = 90; γ, EC_{50} = 0.013 μM, %max = 103) than **10** (α, EC_{50} = 0.623 μM, %max = 52; γ, EC_{50} = 0.140 μM, %max = 94).

We also determined selectivity data over PPARδ for selected compounds **17d**, **17e**, and **17j** in transactivation assays. PPARδ is another member of the PPAR superfamily that is expressed in several tissues and plays an important role in the regulation of lipid metabolism and energy homeostasis.[1,2] No activity was observed for **17d** and **17e**, while **17j** showed only weak activity (EC_{50} = 19 μM) at this PPAR subtype.

As we intended to evaluate selected compounds in vivo using rodent models of type 2 diabetes and dyslipidemia, and since we anticipated a decrease in potency in the transactivation assay when going from human to rodent PPARα based on our experience with **10** (>16-fold decrease),[19] and on several other reports with a variety of agonists,[28–34] **17d**, **17i**, and **17j** were selected for evaluation in transactivation assays using rat PPARα and mouse PPARγ. No activation of rat PPARα was observed with **17d**, while **17i** and **17j** showed weak activation (EC_{50} = 4.1 μM and EC_{50} = 2.6 μM, respectively). These results confirmed our expectation that a decrease in potency would occur when going from human to rat PPARα, with the most significant drop observed with **17j** (43-fold). Results obtained with mouse PPARγ for **17d**, **17i**, and **17j** (EC_{50} = 0.233 μM, EC_{50} = 0.003 μM, and EC_{50} = 0.003 μM, respectively) were closer to the values observed with human PPARγ (Table 1: **17d**, EC_{50} = 0.228 μM; **17i**, EC_{50} = 0.015 μM; **17j**, EC_{50} = 0.013 μM). These results were in agreement with data from our first report and confirmed that this series of compounds exhibit high selectivity for human PPARα over rat PPARα, while there is hardly any difference between human and mouse PPARγ.

3.1. X-ray crystallography and computational studies

An approximately 10-fold increase in potency for activation of both PPAR α and γ was observed with the replacement of the pyrrole of **10** with the 1,2,3-triazol-2-yl of **17j**. In an attempt to better rationalize this difference in potency through structural information, the structure of the complex of **17j** bound to the human PPARγ-ligand binding domain (LBD) (residues Glu207 to Tyr477) was determined by X-ray crystallography following conditions previously described.[19] The complex structure was determined to 2.30 Å resolution with an *R*-factor of 24.1% and *R*-free of 29.7% (see Supplementary data for X-ray data collection and structure refinement statistics). The interactions between **17j** and the PPARγ LBD highly resemble those previously observed with **10**. Triazole **17j** binds to the activated PPARγ receptor with its carboxylate head group forming a network of hydrogen bonds involving the 'charge clamp' residues His323 and Tyr327 from helix 6, His449 from helix 11, Tyr473 from the activation helix 12 and Ser289 from helix 3 (Fig. 4). The interactions between the central hydrophobic linker and the 5-methyl-2-phenyloxazole tail group of **17j** with PPARγ were also similar to those previously observed with **10**. The linker of **17j** is positioned on top of Cys285 from helix 3 and Met364 from helix 7 and encounters additional hydrophobic residues including Ile326 and Leu330. The phenyloxazole tail reaches the hydrophobic pocket formed by Val339, Ile341, Met348, Ile281 and Leu353. Further examination of the mode of binding of **17j** with the PPARγ LBD revealed a new interaction that was not possible to obtain with **10**. In a unique mode for **17j**, the formation of an additional hydrogen bond between *N*-2 of the triazole ring of **17j** and the imidazole residue of His449 in PPARγ (3.1 Å distance) was observed.

As we did not have access to a crystal structure of our compounds with PPARα, we decided to build a model to gain additional understanding of the interactions of **17j** with PPARα. The complex of **17j** with PPARγ-LBD was superimposed onto the co-crystal structure of the potent, full agonist GW409544 complexed with human PPARα-LBD (Fig. 5).[35] From this model, and as expected for this class of compounds, the carboxylate head group of the ligand engaged in a hydrogen bond network with the charge clamp residues, including Ser280, Tyr314, Tyr464, and His440. Similarly to the interaction with PPARγ, the model showed that an additional hydrogen bond between *N*-2 of the triazole ring of **17j** and the imidazole residue of His440 in PPARα (3.6 Å distance) might be formed. It has been reported that a neutral–neutral hydrogen bond is worth up to 1.5 kcal/mol, which represents a maximum 15-fold increase in binding.[36,37] Taken this into consideration, the binding energy gain with the additional hydrogen bond obtained with the triazole as observed from the crystal structure and predicted from modeling studies provides a plausible explanation for the potency difference between **17j** and **10** for their interaction with both PPARα and PPARγ.

The results obtained with pyrazole **17e** and triazole analogs **17g** and **17h** were intriguing to us. Although all these compounds included a five-membered ring heterocycle at the α-position of the

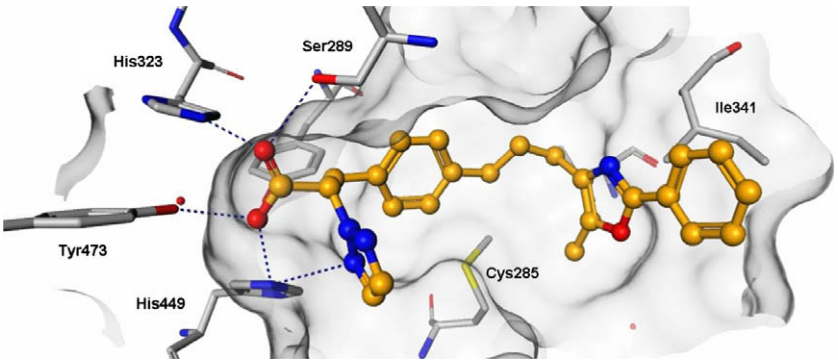

Figure 4. Three-dimensional representation of **17j** (gold ball and stick) bound in the ligand binding pocket of human PPARγ. The figure shows the carboxylate head group of **17j** forming H-bond interactions with the charge clamp residues His323, Tyr473, His449, and Ser289 (gray stick). Formation of an additional H-bond between *N*-2 of the α-triazole ring of **17j** and His449 (3.1 Å distance) was observed from the crystal structure.

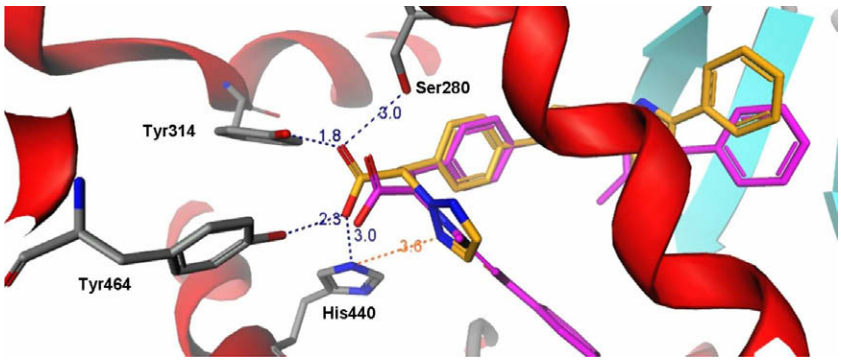

Figure 5. The crystal structure of **17j** (gold stick) bound to human PPARγ (not shown) was superimposed onto the crystal structure of GW409544 (magenta stick) bound to human PPARα (ribbons and β-sheets).[35] The figure shows the carboxylate head group of **17j** forming H-bond interactions (blue dotted lines) with the charge clamp residues Ser280, Tyr314, Tyr464, and His440 (gray sticks). Similarly to the interaction with PPARγ, an additional H-bond (orange dotted line) between *N*-2 of the α-triazole ring of **17j** and His440 of PPARα may form as observed from the distance (3.6 Å) determined from this model.

scaffold that is relatively similar to that in **17j**, and that might be capable of forming the additional hydrogen bond, they all showed a decrease in potency. Both **17g** and **17h** showed drastically lower potency than **17j**, while this compound was approximately five-fold more potent than **17e** (based on EC_{50} values for PPARγ). It was then interesting to attempt to rationalize these findings. The results obtained with isoxazole analogs **17b** and **17c** and triazole analogs **17g** and **17h** suggested that polar five-membered heterocycles with a heteroatom at positions 3 or 4 are not tolerated at the α-position of the scaffold. A high penalty for desolvation of heteroatoms at positions 3 or 4, as well as differences in electron density of the heterocycle that may alter the potential for forming the additional hydrogen bond were considered as plausible explanations for the reduction in potency. In order to further evaluate the latter, electrostatic potential calculations were performed. For simplicity, calculations were performed utilizing 1-methylpyrrole, 1-methylpyrazole, 1-methyl-1,2,4-triazole, 1-methyl-1,2,3-triazole, and 2-methyl-1,2,3-triazole. The electrostatic potential maps of these compounds are graphically displayed in Figure 6. These calculations showed all heterocycles, with the exception of pyrrole, with high negative electrostatic potential at position 2 of the heterocyclic ring that suggests that all may have the potential to form the additional hydrogen bond. Therefore, other possible explanations for the difference in activity were contemplated. As mentioned above, it was observed that heterocycles with a heteroatom at positions 3 or 4 are not tolerated at the α-position of the scaffold. This led us to consider that the bottom end of the heterocycle (positions 3 and 4) might interact with a region of both PPAR subtypes that prefers non-polar groups in this part of the molecule. Examination of the structure of the complex of **17j** bound to human PPARγ-LBD revealed that the bottom end of the triazole ring interacts with Phe282 and Phe363 of PPARγ. Therefore, the drastic

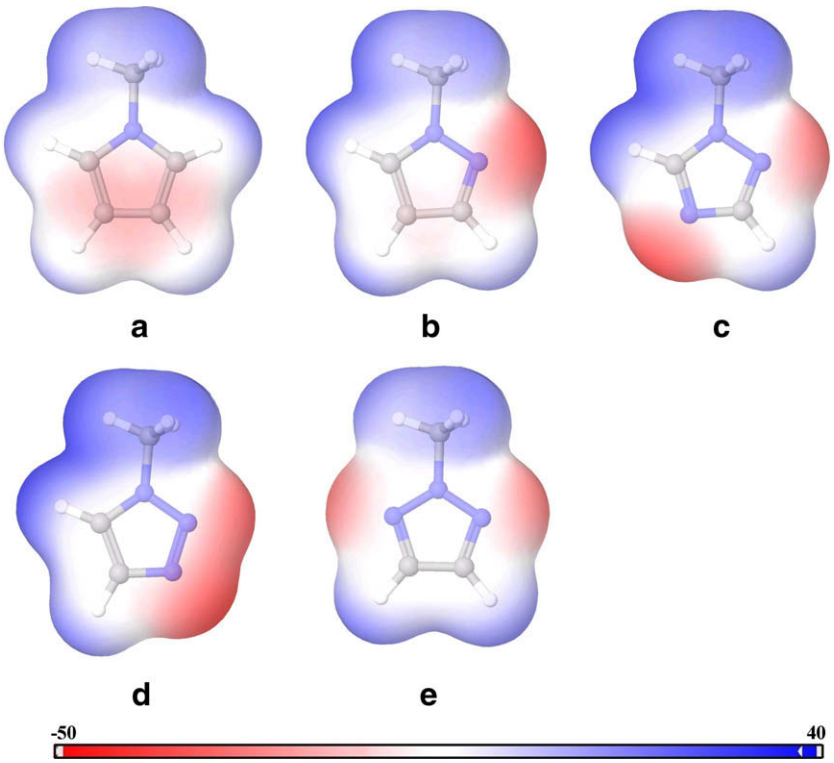

Figure 6. Electrostatic potential maps of five-membered ring heterocycles. Red represents negative potential values and blue indicates positive potential values: (a) 1-methylpyrrole, (b) 1-methylpyrazole, (c) 1-methyl-1,2,4-triazole, (d) 1-methyl-1,2,3-triazole, (e) 2-methyl-1,2,3-triazole.

difference in activity between **17j** and analogs with heterocyclic rings with polar heteroatoms at positions 3 and 4 might be explained by repulsive interactions between the bottom end of the heterocycle and hydrophobic residues in both PPAR subtypes. In the case of **17e**, other explanations were considered. It was already pointed out that although the heterocycle at the α-position of the scaffold in **17e** might be capable of forming the additional hydrogen bond, this compound showed an approximately five-fold change in potency compared to **17j**. This drop in potency might be derived from conformational entropy penalty differences. Due to the symmetry of the triazole ring of **17j**, there are two nitrogens capable of hydrogen-bonding. Then, **17j** might have a lower conformational entropy penalty to form the additional hydrogen bond than **17e** that has only one nitrogen capable of engaging in this interaction.

3.2. Pharmacokinetic and in vivo evaluation

As the next step in this investigation was to perform studies in animal models of diabetes and dyslipidemia, the pharmacokinetic properties of **17j** were evaluated in rat and dog (Table 2) to determine if this compound would be suitable for oral administration. Bioavailability was moderate in rat (42%), while it was high in dog (>95%). Compound **17j** had moderate plasma clearance and volume of distribution in both species (rat: Cl = 18 mL/min/kg, Vss = 2.9 L/kg; dog: Cl = 4.4 mL/min/kg, Vss = 0.82 L/kg). The measured half-life values for **17j** were 7.5 h in rat and and 5.8 h in dog. Although an increase in plasma clearance and volume of distribution was observed when **17j** was compared to **10** (rat: Cl = 5.3 mL/min/kg, Vss = 1.06 L/kg, %*F* = 50), the profile of **17j** was considered appropriate to continue with our research.

A short four-day study with **17j** in the *ob*/*ob* mice, a leptin deficient model of insulin resistance and diabetes,[38] was used to characterize the effects of this compound at low doses (0.01, 0.03, 0.1, 0.3 and 1 mg/kg/day) and to compare its effects to the actions of rosiglitazone at 20 mg/kg/day. This dose selection was based on preliminary studies carried out with the racemic analog **17i** which exhibited lowering of plasma glucose, insulin, and triglycerides levels even at low doses (2 mg/kg/day). At both 0.3 and 1 mg/kg, **17j** demonstrated blood glucose lowering effects similar to those observed with rosiglitazone (Table 3). In addition, treatment with **17j** significantly reduced plasma triglycerides at doses down to 0.1 mg/kg.

To further characterize the effects of **17j**, this compound was then evaluated in the ZDF female rat,[39] a widely used model that has been utilized to demonstrate insulin sensitization. Animals were administered **17j** at a dose of 0.1, 0.3, 1 and 3 mg/kg/day (*n* = 6 animals/group), or rosiglitazone at 3 mg/kg/day for 2 weeks. The results of this study are described in Table 4. Treatment with **17j** at 0.1–3 mg/kg/day normalized glucose and insulin, with maximal reductions present after one week of treatment. Additionally, insulin levels were significantly lowered as compared to the rosiglitazone treated animals (**17j** at 0.3–3 mg/kg/day compared to rosiglitazone at 3 mg/kg/day). As in the *ob*/*ob* mouse model, **17j** significantly lowered triglycerides in the ZDF rat at all dose levels. Additionally, **17j** significantly lowered triglycerides by more than 70% as compared to rosiglitazone (**17j** at 0.3–3 mg/kg/day vs rosiglitazone at 3 mg/kg/day). A decrease in hematocrit, which served as a marker of hemodilution (indicator of plasma volume expansion resulting from fluid retention),[40] was observed in a dose proportional manner upon treatment with **17j** (Table 4). In addition, an approximately 20% increase in body weight was observed upon treatment with **17j** (Table 4) at all doses when compared to the vehicle control. We have previously observed body weight increases with **10** when compared to control (31% at a dose of 10 mg/kg/day for 4 weeks) in this preclinical model. While body weight gain is a well known side effect of PPARγ activation, body weight reduction in rodents has been reported with the PPARα agonists fenofibrate,[41] and oleoylethanolamide and its derivatives.[42] We have previously hypothesized that **10** does not possess the PPARα activity sufficient to counterbalance the PPARγ-mediated body weight gain. The profile observed with **17j** allowed us to assess if higher agonist efficacy for human PPARα with respect to **10**, would provide an improvement in reducing body weight gain. Due to the approximately equal increases in potency for both human PPARα and PPARγ obtained with **17j**, we could not assess if selectively increasing potency for the α-subtype would provide benefits for ameliorating body weight gain. In addition, the lower potency of **17j** for rat PPARα (43-fold drop in potency versus human PPARα) might alter the balance of activity between the two PPAR subtypes in rat. Based on our results, the profile obtained with **17j** did not have an effect in reducing body weight gain. It is likely that the effects observed in the ZDF rat model are mainly mediated by PPARγ activation with little or no beneficial effects from PPARα activation.

We next sought to evaluate changes in HDL cholesterol (HDL-C) and serum triglycerides derived from PPAR-mediated effects of **17j** using the human apolipoprotein A-1/CETP transgenic mouse model. Compounds that activate PPARα significantly increase ApoA1 and HDL-C in this model. In a dose ranging study, **17j** produced dose-dependent increase in HDL-C and decrease in plasma triglycerides, while hApoA1 was only increased at the highest dose (Table 5). HDL-C was elevated by 90% at a dose of 3 mg/kg, while triglycerides were decreased by approximately 40% at the same dose. Effects on hApoA1 were only evident at the highest dose of **17j** (10 mg/kg).

A lack of correlation was identified between the effective doses for the in vivo effects of **17j** in the ZDF rat and in the hApoA1 mouse which might be rationalized by taking into account the above discussed species-specific differences for transactivation of PPARα[27–30] among other possible reasons: **17j** exhibits high selectivity (43-fold) for human PPARα over rat PPARα. Pivotal species-specific structural variations within the PPARα-LBD have been used to explain these discrepancies by other groups and are likely responsible for the lack of correlation observed with **17j**.[29,30] The apparent discrepancy in triglyceride lowering is likely due to dif-

Table 2
Pharmacokinetic properties of **17j** in rat and dog

Species	Route	Dose (mg/kg)	AUC (ng h/mL)	$t_{1/2}$ (h)	*F* (%)	Cl (mL/min/kg)	Vss (L/Kg)
Rat	IV	1	928	7.5		18	2.9
	PO	3	1170		42		
Dog	IV	1	3970	5.8		4.4	0.82
	PO	3	13,000		>95		

Table 3
Evaluation of **17j** in *ob*/*ob* mice for four days[a]

Treatment	Dose (mg/kg/day)	Glucose (mg/dL)	Insulin (ng/mL)	Triglycerides (mg/dL)
Vehicle		476 ± 27[c]	21.28 ± 7.5[c]	344 ± 31[c]
Rosiglitazone	20[d]	330 ± 42[b]	5.87 ± 2.1[b]	107 ± 20[b]
17j	0.01	371 ± 34[b]	16.93 ± 5.0	247 ± 47
	0.03	388 ± 44	12.56 ± 4.6	271 ± 55
	0.1[d]	375 ± 43[b]	16.04 ± 2.4	131 ± 21[b]
	0.3	268 ± 17[b]	8.3 ± 1.8[b]	117 ± 25[b]
	1	325 ± 35[b]	3.6 ± 0.6[b]	122 ± 21[b]

[a] All data mean ± SEM, *n* = 6/group.
[b] Significantly different from Vehicle group, $p < 0.05$.
[c] Significantly different from rosiglitazone, $p < 0.05$.
[d] *n* = 5/Group.

Table 4
Evaluation of **17j** in female ZDF rats[a]

Treatment	Dose (mg/kg/day)	Glucose (mg/dL)	Insulin (ng/mL)	Triglycerides (mg/dL)	BW change[b] (%)	Hematocrit change[b] (%)
Vehicle		433 ± 37[c]	20 ± 3[c]	1579 ± 244[c]	—	—
Rosiglitazone	3	154 ± 5[b]	4 ± 0.39[b]	931 ± 107[b]	+14	−5.8
17j	0.1	188 ± 32[b]	3 ± 0.64[b]	846 ± 85[b,c]	+21	−11.6
	0.3	171 ± 11[b]	1.26 ± 0.05[b,c]	252 ± 22[b,c]	+17	−11.1
	1	148 ± 10[b]	1.38 ± 0.28[b,c]	170 ± 13[b,c]	+16	−20
	3	163 ± 8[b]	1.18 ± 0.13[b,c]	191 ± 17[b,c]	+20	−23.7

[a] All data mean ± sem, $n = 6$/group. Tested compounds were administered orally once a day for 2 weeks.
[b] Significantly different from Vehicle group, $p < 0.05$.
[c] Significantly different from rosiglitazone, $p < 0.05$.

Table 5
Evaluation of **17j** in hApoA1 mice[a]

Treatment	Dose (mg/kg/day)	hApoA1 (mg/dL)	HDL-C (mg/dL)	Triglycerides (mg/dL)
Vehicle		700 ± 69	204 ± 7	91 ± 8.2
17j	0.1	713 ± 66 (2)	199 ± 14 (−2)	95 ± 6.2 (4)
	0.3	700 ± 44 (0)	233 ± 9.8 (14)	77 ± 10 (−15)
	1.0	716 ± 52 (2)	283 ± 11 (28)[b]	72 ± 10 (−21)
	3.0	758 ± 60 (8)	388 ± 9.3 (90)[b]	56 ± 4.9 (−39)[b]
	10.0	1018 ± 120 (45)[b]	395 ± 13 (94)[b]	29 ± 4.0 (−69)[b]

[a] All data mean ± SEM (% from control), $n = 6$/group. Tested compounds were administered orally once a day for 14 days.
[b] Significantly different from within study Vehicle group, $p < 0.05$.

ferences in baseline lipids between the hyperlipidemic ZDF rat and the normolipidemic ApoA1 transgenic mouse. Greater hypolipidemic activity is often observed with PPAR modulators using in vivo models that exhibit extreme elevations in their circulating lipid context.

4. Conclusions

This investigation was focused at the identification of novel PPARα/γ dual agonists possessing PPARγ potency similar to that of **10**, a compound recognized as the most potent in our previous series, but endowed with increased PPARα potency in binding and activation assays. Thus, we intended to obtain compounds with a γ:α ratio similar, or even more balanced compared to **10**. We also sought to identify compounds with pharmacokinetic properties suitable for oral administration. Two key elements were used in the design of the new compounds: the incorporation of a propyl linker between the central phenyl ring and the lipophilic tail, and a five-membered ring heterocycle at the α-position of the phenylpropanoic acid scaffold. From these efforts, **17j** containing a 1,2,3-triazol-2-yl moiety at the α-position was identified. This compound showed an approximately 10-fold improvement in potency for activation of PPARα and higher agonist efficacy when compared to **10**, although potency was also increased for PPARγ. Thus, **17j** maintained a similar γ:α ratio to that of **10**. The increased potency obtained with **17j** was rationalized based on crystallography and modeling studies, and was ascribed to the formation of a hydrogen bond between *N*-2 of the triazole ring and the imidazole residue of His449 in PPARγ, or His440 in PPARα, respectively. The pharmacokinetic profile of **17j** in rat was found to be suitable for oral adminstration. **17j** was shown to decrease insulin levels, plasma glucose, and triglycerides in the ZDF female rat model. In the human apolipoprotein A-1/CETP transgenic mouse model **17j** produced dose-dependent increase in HDL-C and decrease in plasma triglycerides, while hApoA1 was only increased at the highest dose. As such, **17j** represented an improvement in this series of phenylpropanoic acids.

5. Experimental section

5.1. General chemistry

All chemicals, reagents and solvents were purchased from commercial sources (e.g., Aldrich Chemical Co., Inc., Milwaukee, WI; Mallinckrodt Baker, Inc., Paris, KY, etc.) where available and used without further purification. All intermediates were characterized by proton nuclear magnetic resonance spectroscopy (^{1}H NMR) and mass spectrometry (MS) using atmospheric pressure chemical ionization (CI) sources. All final compounds were determined to be consistent with the proposed structure by ^{1}H NMR, MS. Elemental analysis was obtained for all final compounds and values were within ±0.4% of the calculated composition. Melting points were determined in capillary tubes and are uncorrected.

5.1.1. *N*-(1-Acetylbut-3-enyl)benzamide (12)

Amide **11** (2.098 g, 11.839 mmol) was dissolved in THF (120 mL) and cooled to −78 °C under nitrogen. A 1.0 M solution of LHMDS in THF (11.9 mL, 11.9 mmol) was added and the mixture stirred for 40 min. A solution of allyl bromide (1.33 mL, 15.39 mmol) in THF (10 mL) was added. The mixture was allowed to warm to rt and stirred overnight. The mixture was diluted with brine and the phases were separated. The aqueous phase was extracted with ethyl acetate (3 × 50 mL) and the combined organic extracts were dried over $MgSO_4$, filtered, and the solvent removed. Purification by flash chromatography on silica gel eluting with hexane/ethyl acetate (2:1–1:1) gave amide **12** (2.02 g, 78%): ^{1}H NMR ($CDCl_3$, 400 MHz) δ 7.79 (d, J = 7.1 Hz, 2H), 7.51–7.41 (m, 3H), 6.95 (br d, J = 5.4 Hz, 1H), 5.74–5.64 (m, 1H), 5.17–5.12 (m, 2H), 4.88 (dt, J = 6.8, 5.4 Hz, 1H), 2.85–2.78 (m, 1H), 2.61–2.54 (m, 1H), 2.28 (s, 3H); CIMS *m/z* 218 $(M+H)^+$. Anal. Calcd for $C_{13}H_{15}NO_2$: C, 71.87; H, 6.96; N, 6.45. Found: C, 71.91; H, 7.03; N, 6.52.

5.1.2. 5-Methyl-2-phenyl-4-prop-2-enyloxazole (13)

Amide **12** (2.00 g, 9.205 mmol) was dissolved in TFA (16 mL) and TFAA (8 mL) was added. The mixture was heated at 35–40 °C for 16 h. The mixture was allowed to cool and the solvents removed under reduced pressure. The residue was diluted with saturated $NaHCO_3$ (50 mL) and solid $NaHCO_3$ was added to neutralize the mixture. It then was extracted with ethyl acetate (3 × 60 mL). The combined organic extracts were washed with brine, dried over $MgSO_4$, filtered and the solvent removed. Purification by flash chromatography on silica gel eluting with hexane/ethyl acetate (15:1) gave oxazole **13** (1.75 g, 95%): ^{1}H NMR ($CDCl_3$, 400 MHz) δ 7.98 (d, J = 7.8 Hz, 2H), 7.43–7.35 (m, 3H), 6.03–5.93 (m, 1H), 5.13 (dq, J = 16.9, 1.7 Hz, 1H), 5.09 (dq, J = 10.0 and 1.5 Hz, 1H), 3.29 (d, J = 6.3 Hz, 2H), 2.32 (s, 3H); CIMS *m/z* 200 $(M+H)^+$.

5.1.3. 3-{4-[3-(5-Methyl-2-phenyl-oxazol-4-yl)-propyl]-phenyl}-2-pyridin-3-yl-propionic acid (17a)

5.1.3.1. Step 1: 3-(4-Bromo-phenyl)-2-thiophen-3-yl-propionic acid ethyl ester (15a). *General method I:* Thiophen-3-yl-acetic acid ethyl ester (1.5 mL, 9.986 mmol) was dissolved in dry THF (15 mL) and cooled to −78 °C under a nitrogen atmosphere. A 1.0 M solution of LHMDS in THF (11 mL, 11 mmol) was added. The mixture was stirred at −78 to −40 °C for 1.25 h. A solution of 4-chlorobenzyl bromide (2.46 g, 11.983 mmol) in THF (5 mL) was added. The reaction was allowed to reach room temperature overnight. The mixture was quenched with water (40 mL) and diluted with EtOAc (30 mL). The phases were separated and the aqueous phase was extracted with EtOAc (3 × 35 mL). The combined organic extracts were washed with brine, dried over magnesium sulfate and the solvent removed. Purification by column chromatography on silica gel eluting with ethyl acetate in hexanes (0–5%) afforded bromide **15a** as an oil (3.195 g, 94%): ^{1}H NMR ($CDCl_3$, 400 MHz) δ 7.35 (d, J = 8.3 Hz, 2H), 7.30–7.25 (m, 1H), 7.09 (d, J = 3.9 Hz, 1H), 7.04 (d, J = 4.9 Hz, 1H), 6.98 (d, J = 8.5 Hz, 2H), 4.12–4.04 (m, 2H), 3.92 (dd, J = 8.5, 6.8 Hz, 1H), 3.27 (dd, J = 13.7, 8.5 Hz, 1H), 2.98 (dd, J = 13.7, 6.8 Hz, 1H), 1.15 (t, J = 7.1 Hz, 3H); CIMS m/z 339.0 $(M)^+$.

5.1.3.2. Step 2: 3-{4-[3-(5-Methyl-2-phenyl-oxazol-4-yl)-propyl]-phenyl}-2-thiophen-3-yl-propionic acid ethyl ester (16a). *General method II:* A solution of 5-methyl-2-phenyl-4-prop-2-enyloxazole (**13**) (0.40 g, 2.007 mmol) in dry THF (6 mL) was added to a solution of 9-BBN in THF (0.5 M, 8.03 mL, 4.015 mmol) at 0 °C under a nitrogen atmosphere. The ice bath was removed and the mixture was stirred at room temperature overnight. The 9-BBN adduct was then added to a flask containing bromide **15a** (0.523 g, 1.544 mmol), $PdCl_2$(dppf) (0.112 g, 0.154 mmol), Cs_2CO_3 (0.905 g, 2.779 mmol), Ph_3As (0.047 g, 0.154 mmol), water (0.333 mL, 18.528 mmol) and DMF (6 mL). The reaction mixture was stirred at room temperature under a nitrogen atmosphere overnight. The mixture was cooled in an ice bath and 3 M NaOAc (12 mL) was added followed by 30% hydrogen peroxide (6 mL). Stirring was continued for 2 h, allowing the reaction to warm to room temperature slowly. Water (50 mL) was added followed by diethyl ether (35 mL). The phases were separated and the aqueous phase was extracted with diethyl ether–ethyl acetate (30:5 mL × 4). The combined organic extracts were washed with brine, dried over magnesium sulfate and the solvent removed. Purification by column chromatography on silica gel eluting with ethyl acetate in hexanes (0–14%) afforded ester **16a** as a thick oil (0.555 g, 78%): ^{1}H NMR ($CDCl_3$, 400 MHz) δ 7.91 (d, J = 8.3 Hz, 2H), 7.35–7.33 (m, 3H), 7.09 (d, J = 8.0 Hz, 1H), 7.04–6.94 (m, 6H), 4.04–3.98 (m, 2H), 3.88 (dd, J = 8.8, 6.6 Hz, 1H), 3.22 (dd, J = 13.7, 9.0 Hz, 1H), 2.96 (dd, J = 13.7, 6.8 Hz, 1H), 2.55 (t, J = 7.6 Hz, 2H), 2.42 (t, J = 7.6 Hz, 2H), 2.20 (s, 3H), 1.90 (qn, J = 7.8 Hz, 2H), 1.07 (t, J = 7.1 Hz, 3H); CIMS m/z 460.2 (M+1).

5.1.3.3. Step 3: 3-{4-[3-(5-Methyl-2-phenyl-oxazol-4-yl)-propyl]-phenyl}-2-pyridin-3-yl-propionic acid (17a). *General method III:* Ester **16a** (0.356 g, 0.774 mmol) was dissolved in THF (25 mL) and water was added (8 mL) followed by LiOH monohydrate (0.162 g, 3.87 mmol). The mixture was stirred for 5 h at room temperature. The solvent was removed and the residue diluted with water and acidified with 10% HCl. The product was extracted with chloroform (4 × 30 mL). The combined organic extracts were washed, dried over magnesium sulfate and the solvent removed. Purification by chromatography on silica gel eluting with ethyl acetate in hexanes (0–45%) gave acid **17a** as a solid (0.193 g, 58%): mp 112–114 °C; ^{1}H NMR ($CDCl_3$, 400 MHz) δ 7.74–7.72 (m, 2H), 7.47–7.32 (m, 3H), 7.21 (d, J = 8.0 Hz, 1H), 7.09–6.93 (m, 6H), 3.92 (dd, J = 8.8, 6.6 Hz, 1H), 3.24 (dd, J = 13.9, 8.8 Hz, 1H), 2.97 (dd, J = 13.9, 6.8 Hz, 1H), 2.52 (t, J = 6.6 Hz, 2H), 2.41 (t, J = 6.6 Hz, 2H), 1.86 (qn, J = 8.0 Hz, 2H); CIMS m/z 432.1 (M+1). Anal. Calcd for $C_{26}H_{25}NO_3S$: C, 72.36; H, 5.84; N, 3.25. Found: C, 72.18; H, 5.97; N, 3.04.

5.1.4. 2-(5-Methyl-isoxazol-3-yl)-3-{4-[3-(5-methyl-2-phenyl-oxazol-4-yl)-propyl]-phenyl}-propionic acid (17b)

5.1.4.1. Step 1: 3-(4-Bromo-phenyl)-2-(5-methyl-isoxazol-3-yl)-propionic acid ethyl ester (15b). Prepared from (5-methyl-isoxazol-3-yl)-acetic acid ethyl ester (2.0 g, 11.82 mmol) following the general method I. Purification by column chromatography on silica gel eluting with ethyl acetate in hexanes (0–10%) gave ester **15b** as a thick oil (3.39 g, 56%): ^{1}H NMR ($CDCl_3$, 400 MHz) δ 7.37 (d, J = 8.3 Hz, 2H), 7.04 (d, J = 8.5 Hz, 2H), 6.00 (s, 1H), 4.13–4.06 (m, 2H), 4.03 (t, J = 7.1 Hz, 1H), 3.27 (dd, J = 13.9, 8.8 Hz, 1H), 3.07 (dd, J = 13.9, 7.1 Hz, 1H), 2.39 (s, 3H), 1.15 (t, J = 7.1 Hz, 3H); CIMS m/z 338.0 $(M)^+$.

5.1.4.2. Step 2: 2-(5-Methyl-isoxazol-3-yl)-3-{4-[3-(5-methyl-2-phenyl-oxazol-4-yl)-propyl]-phenyl}-propionic acid ethyl ester (16b). Prepared from bromide **15b** (1.0 g, 2.956 mmol) following general method II. Purification by column chromatography on silica gel eluting with ethyl acetate in hexanes (0–16%) afforded ester **16b** as a thick oil (1.14 g, 84%): ^{1}H NMR ($CDCl_3$, 400 MHz) δ 8.03–7.98 (m, 2H), 7.45–7.40 (m, 3H), 7.07 (d, J = 7.6 Hz, 2H), 7.06 (d, J = 7.8 Hz, 2H), 6.00 (s, 1H), 4.10–4.03 (m, 3H), 3.26 (dd, J = 13.9, 8.8 Hz, 1H), 3.06 (dd, J = 13.7, 6.8 Hz, 1H), 2.61 (t, J = 7.6 Hz, 2H), 2.51 (t, J = 7.6 Hz, 2H), 2.37 (s, 3H), 2.26 (s, 3H), 1.98 (qn, J = 7.8 Hz, 2H), 1.12 (t, J = 7.1 Hz, 3H); CIMS m/z 459.3 (M+1).

5.1.4.3. Step 3: 2-(5-Methyl-isoxazol-3-yl)-3-{4-[3-(5-methyl-2-phenyl-oxazol-4-yl)-propyl]-phenyl}-propionic acid (17b). Prepared from ester **16b** (1.093 g, 2.384 mmol) following general method III. Purification by chromatography on silica gel eluting with methanol in chloroform (0–3%) provided acid **17b** as a solid (0.950 g, 93%): mp 130–133 °C; ^{1}H NMR ($CDCl_3$, 400 MHz) δ 7.97–7.94 (m, 2H), 7.41–7.38 (m, 3H), 7.09 (d, J = 8.0 Hz, 2H), 7.04 (d, J = 8.3 Hz, 2H), 6.00 (s, 1H), 4.11 (dd, J = 8.5, 6.8 Hz, 1H), 3.30 (dd, J = 13.9, 8.8 Hz, 1H), 3.10 (dd, J = 13.9, 6.8 Hz, 1H), 2.56 (t, J = 7.6 Hz, 2H), 2.47 (t, J = 7.6 Hz, 2H), 2.36 (s, 3H), 2.25 (s, 3H), 1.91 (qn, J = 7.6 Hz, 2H); CIMS m/z 431.2 (M+1). Anal. Calcd for $C_{26}H_{26}N_2O_4$: C, 72.54; H, 6.09; N, 6.51. Found: C, 72.42; H, 6.29; N, 6.33.

5.1.5. 2-(3-Methyl-isoxazol-5-yl)-3-{4-[3-(5-methyl-2-phenyl-oxazol-4-yl)-propyl]-phenyl}-propionic acid (17c)

5.1.5.1. Step 1: 3-(4-Bromo-phenyl)-2-(3-methyl-isoxazol-5-yl)-propionic acid ethyl ester (15c). This compound was prepared from 3-methyl-isoxazol-5-yl-acetic acid methyl ester following the general method I. Bromide **15c** was obtained as a thick oil in 34% yield: ^{1}H NMR ($CDCl_3$, 400 MHz) δ 7.37 (d, J = 8.5 Hz, 2H), 6.99 (d, J = 8.5 Hz, 2H), 5.96 (s, 1H), 4.06 (t, J = 7.6 Hz, 1H), 3.67 (s, 3H), 3.28 (dd, J = 13.9, 8.0 Hz, 1H), 3.16 (dd, J = 13.7, 7.3 Hz, 1H), 2.25 (s, 3H); CIMS m/z 324.0 $(M)^+$.

5.1.5.2. Step 2: 2-(3-Methyl-isoxazol-5-yl)-3-{4-[3-(5-methyl-2-phenyl-oxazol-4-yl)-propyl]-phenyl}-propionic acid methyl ester (16c). This compound was prepared following the general method II using bromide **15c** for the Suzuki coupling. Ester **16c** was obtained as thick oil in 60% yield: ^{1}H NMR ($CDCl_3$, 400 MHz) δ 8.02–7.99 (m, 2H), 7.44–7.40 (m, 3H), 7.08 (d, J = 8.3 Hz, 2H), 7.01 (d, J = 8.1 Hz, 2H), 5.96 (s, 1H), 4.06 (t, J = 7.6 Hz, 1H), 3.64 (s, 3H), 3.28 (dd, J = 13.7, 8.1 Hz, 1H), 3.15 (dd, J = 13.9, 7.3 Hz,

1H), 2.61 (t, *J* = 7.3 Hz, 2H), 2.51 (t, *J* = 7.3 Hz, 2H), 2.26 (s, 3H), 2.24 (s, 3H), 1.98 (qn, *J* = 7.6 Hz, 2H); CIMS *m/z* 459.3 (M+1).

5.1.5.3. Step 3: 2-(3-Methyl-isoxazol-5-yl)-3-{4-[3-(5-methyl-2-phenyl-oxazol-4-yl)-propyl]-phenyl}-propionic acid (17c). This compound was prepared from ester **16c** following Method III. The purification was carried out by chromatography on silica gel eluting with methanol in chloroform (0–5%). Acid **17c** was obtained as an off-white solid in 85% yield: mp 133–135 °C; ^{1}H NMR ($CDCl_3$, 400 MHz) δ 7.98–7.95 (m, 2H), 7.42–7.39 (m, 3H), 7.07 (d, *J* = 8.3 Hz, 2H), 7.04 (d, *J* = 8.3 Hz, 2H), 6.01 (s, 1H), 4.11 (t, *J* = 8.1 Hz, 1H), 3.30 (dd, *J* = 13.9, 8.5 Hz, 1H), 3.18 (dd, *J* = 13.9, 7.1 Hz, 1H), 2.56 (t, *J* = 7.6 Hz, 2H), 2.48 (t, *J* = 7.6 Hz, 2H), 2.26 (s, 3H), 2.24 (s, 3H), 1.90 (qn, *J* = 7.6 Hz, 2H); CIMS *m/z* 431.2 (M+1). Anal. Calcd for $C_{26}H_{26}N_2O_4$: C, 72.54; H, 6.09; N, 6.51. Found: C, 72.32; H, 6.28; N, 6.41.

5.1.6. 3-{4-[3-(5-Methyl-2-phenyl-oxazol-4-yl)-propyl]-phenyl}-2-pyrazol-1-yl-propionic acid (17d)

5.1.6.1. Step 1: Ethyl 3-(4-bromophenyl)-2-(1*H*-pyrazol-1-yl)propanoate (15d). Prepared from pyrazol-1-yl acetic acid ethyl ester (10.0 g, 64.86 mmol) following general method I. Bromide **15d** was obtained as a clear, thick oil (9.73 g, 46%): ^{1}H NMR ($CDCl_3$, 400 MHz) δ 7.53 (d, *J* = 1.7 Hz, 1H), 7.36 (d, *J* = 2.0 Hz, 1H), 7.33 (d, *J* = 8.5 Hz, 2H), 6.88 (d, *J* = 8.3 Hz, 2H), 5.05 (dd, *J* = 8.8, 6.6 Hz, 1H), 4.18 (dd, *J* = 14.2, 7.1 Hz, 2H), 3.49–3.39 (m, 2H), 1.20 (t, *J* = 7.1 Hz, 3H); CIMS *m/z* 323 $(M)^+$.

5.1.6.2. Step 2: 3-{4-[3-(5-Methyl-2-phenyl-oxazol-4-yl)-propyl]-phenyl}-2-pyrazol-1-yl-propionic acid ethyl ester (16d). Prepared from bromide **15d** (0.760 g, 2.351 mmol) by the general method II. Purification by column chromatography afforded **16d** (0.735 g, 70%): ^{1}H NMR ($CDCl_3$, 400 MHz) δ 7.98–7.95 (m, 2H), 7.52 (d, *J* = 1.5 Hz, 1H), 7.44–7.38 (m, 4H), 7.05 (d, *J* = 8.0 Hz, 2H), 6.94 (d, *J* = 8.0 Hz, 2H), 6.22 (t, *J* = 2.1 Hz, 1H), 5.11 (t, *J* = 7.7 Hz, 1H), 4.16 (q, *J* = 7.1 Hz, 2H), 3.43 (d, *J* = 7.8 Hz, 2H), 2.60 (t, *J* = 7.6 Hz, 2H), 2.47 (t, *J* = 7.3 Hz, 2H), 2.26 (s, 3H), 1.95 (qn, *J* = 7.8 Hz, 2H), 1.18 (t, *J* = 7.1 Hz, 3H); CIMS *m/z* 444 (M+1).

5.1.6.3. Step 3: 3-{4-[3-(5-Methyl-2-phenyl-oxazol-4-yl)-propyl]-phenyl}-2-pyrazol-1-yl-propionic acid (17d). Prepared from ester **16d** (0.735 g, 1.657 mmol) by the general method III. Acid **17d** was obtained as a yellowish solid (0.602 g, 87%): mp 75–77 °C; ^{1}H NMR ($CDCl_3$, 400 MHz) δ 7.96 (m, 2H), 7.61 (d, *J* = 2.0 Hz, 1H), 7.40 (m, 3H), 7.09 (d, *J* = 2.0 Hz, 1H), 7.02 (d, *J* = 8.0 Hz, 2H), 6.80 (d, *J* = 8.0 Hz, 2H), 6.19 (t, *J* = 2.2 Hz, 1H), 5.02 (dd, *J* = 10.0, 4.6 Hz, 1H), 3.42 (dd, *J* = 13.9, 4.6 Hz, 1H), 3.27 (dd, *J* = 13.9, 10.0 Hz, 1H), 2.59 (t, *J* = 7.6 Hz, 2H), 2.47 (t, *J* = 7.6 Hz, 2H), 2.27 (s, 3H), 1.93 (m, 2H); CIMS *m/z* 416 (M+1). Anal. Calcd for $C_{25}H_{25}N_3O_3 \cdot 0.4H_2O$: C, 71.04; H, 6.15; N, 9.94. Found: C, 70.76; H, 6.08; N, 9.91.

5.1.7. (*S*)-3-{4-[3-(5-Methyl-2-phenyl-oxazol-4-yl)-propyl]-phenyl}-2-pyrazol-1-yl-propionic acid (17e)

The enantiomers of acid **17d** (10.1 g) were separated by preparative chiral HPLC: chiralpak AD column, 4.6 × 250 mm; mobile phase A: 75% hexanes with 0.1% trifluoroacetic acid; mobile phase B; 25% ethanol; flow rate: 1 mL/min; detection at 280 nm. Compound **17e** was obtained as a pale yellowish solid (4.06 g): mp 115–117 °C; $[\alpha]_D^{25} = -57.0$ (*c* 1.47, THF); ^{1}H NMR and MS were identical to racemate. Enantiomer purity: 98.1%, retention time = 6.48 min. Anal. Calcd for $C_{25}H_{25}N_3O_3 \cdot 0.29CHCl_3$: C, 67.48; H, 5.66; N, 9.34. Found: C, 67.09; H, 5.63; N, 9.19.

5.1.8. (*R*)-3-{4-[3-(5-Methyl-2-phenyl-oxazol-4-yl)-propyl]-phenyl}-2-pyrazol-1-yl-propionic acid (17f)

This compound was obtained from the above purification. Acid **17f** was obtained as a pale yellow solid (4.17 g): $[\alpha]_D^{25} = +61.0$ (*c* = 1.22, THF); mp 124–127 °C; ^{1}H NMR and MS were identical to racemate. Enantiomer purity: 98.35%, retention time = 8.12 min.

5.1.9. 3-{4-[3-(5-Methyl-2-phenyl-oxazol-4-yl)-propyl]-phenyl}-2-1,2,4-triazol-1-yl-propionic acid (17g)

5.1.9.1. Step 1: Ethyl 3-(4-bromophenyl)-2-(1H-1,2,4-triazol-1-yl)propanoate (15g). *General method IV*. A solution of diisopropyl amine (1.0 mL, 7.089 mmol) in dry diethyl ether (10 mL) was cooled to −20 °C under a nitrogen atmosphere. A solution of *n*-BuLi in hexanes (1.6 M, 4.8 mL, 7.734 mmol) was added. Mixture stirred for 20 min. A solution of ethyl 2-1,2,4-triazol-1-yl acetate (1.0 g, 6.445 mmol) in diethyl ether (10 mL) was added and this was followed by the addition of a solution of 4-bromobenzyl bromide (1.61 g, 6.445 mmol) in diethyl ether (20 mL). The mixture was stirred at −20 °C for 4 h, then allowed to reach room temperature and stirred overnight. Mixture was quenched with water and the phases were separated. Aqueous phase was acidified with 10% HCl and extracted with ethyl acetate (3 × 35 mL). The combined organic extracts were washed with water, brine, dried over $MgSO_4$, filtered, and the solvent removed. Purification by flash chromatography on silica gel eluting with ethyl acetate in hexanes (0–45%) gave bromide **15g** as a thick oil (0.447 g, 21%): ^{1}H NMR ($CDCl_3$, 400 MHz) δ 8.10 (s, 1H), 7.98 (s, 1H), 7.35 (d, *J* = 8.3 Hz, 2H), 6.86 (d, *J* = 8.5 Hz, 2H), 5.16 (dd, *J* = 8.1, 6.7 Hz, 1H), 4.22 (q, *J* = 7.1 Hz, 2H), 3.46 (d, *J* = 7.6 Hz, 2H), 1.23 (t, *J* = 7.1 Hz, 3H); CIMS *m/z* 324 $(M)^+$.

5.1.9.2. Step 2: 3-{4-[3-(5-Methyl-2-phenyl-oxazol-4-yl)-propyl]-phenyl}-2-1,2,4-triazol-1-yl-propionic acid ethyl ester (16g). Prepared from bromide **15g** (0.440 g, 1.357 mmol) following general method II. Ester **16g** was obtained as a thick oil (0.492 g, 82%): ^{1}H NMR ($CDCl_3$, 400 MHz) δ 8.09–8.07 (m, 2H), 8.00 (s, 1H), 7.94 (s, 1H), 7.48–7.41 (m, 3H), 7.06 (d, *J* = 8.0 Hz, 2H), 6.88 (d, *J* = 8.0 Hz, 2H), 5.17 (dd, *J* = 8.0, 6.6 Hz, 1H), 4.21 (q, *J* = 7.1 Hz, 2H), 3.43 (d, *J* = 7.3 Hz, 2H), 2.62 (t, *J* = 7.6 Hz, 2H), 2.53 (t, *J* = 7.3 Hz, 2H), 2.28 (s, 3H), 1.99 (qn, *J* = 7.8 Hz, 2H), 1.23 (t, *J* = 7.1 Hz, 3H); CIMS *m/z* 445 (M+1).

5.1.9.3. Step 3: 3-{4-[3-(5-Methyl-2-phenyl-oxazol-4-yl)-propyl]-phenyl}-2-1,2,4-triazol-1-yl-propionic acid (17g). Prepared from ester **16g** (0.492 g, 1.106 mmol) following general method III. Acid **17g** was obtained as a white solid (0.33 g, 72%): mp 169–171 °C; ^{1}H NMR ($CDCl_3$, 400 MHz) δ 8.16 (s, 1H), 8.02-7.99 (m, 2H), 7.98 (s, 1H), 7.45–7.40 (m, 3H), 7.01 (d, *J* = 8.0 Hz, 2H), 6.87 (d, *J* = 8.0 Hz, 2H), 5.24 (t, *J* = 7.1 Hz, 1H), 3.42 (d, *J* = 7.1 Hz, 2H), 2.57 (t, *J* = 7.6 Hz, 2H), 2.52 (t, *J* = 7.6 Hz, 1H), 3.42 (d, *J* = 7.1 Hz, 2H), 2.57 (t, *J* = 7.6 Hz, 2H), 2.51 (t, *J* = 7.6 Hz, 2H), 2.28 (s, 3H), 1.93 (qn, *J* = 7.6 Hz, 2H); CIMS *m/z* 417 (M+1). Anal. Calcd for $C_{24}H_{24}N_4O_3 \cdot 0.2H_2O$: C, 68.62; H, 5.85; N, 13.34. Found: C, 68.51; H, 5.85; N, 13.26.

5.1.10. 3-{4-[3-(5-Methyl-2-phenyl-oxazol-4-yl)-propyl]-phenyl}-2-1,2,3-triazol-1-yl-propionic acid (17h)

5.1.10.1. Step 1: Ethyl 2-(1*H*-1,2,3-triazol-1-yl)acetate (14h). Prepared following the procedure described by Kume et al.[43] Following this procedure, starting from 1*H*-1,2,3-triazole (18.17 g, 0.263 mol), the *N*-1 alkylated product **14h** was obtained as a liquid (26.45 g, 65%) after purification by column chromatography on silica gel eluting with ethyl acetate in hexanes (0 to 55%): ^{1}H NMR ($CDCl_3$, 400 MHz) δ 7.75 (d, *J* = 1.0 Hz, 1H), 7.71 (d, *J* = 1.0 Hz, 1H), 5.19 (s, 2H), 4.25 (q, *J* = 7.1 Hz, 2H), 1.28 (t, *J* = 7.1 Hz, 3H); CIMS *m/z* 156 (M+1).

*2-(2H-1,2,3-Triazol-2-yl)ethyl acetate (**14i**)*: From the same purification, ester **14i** was obtained as a liquid (9.2 g, 22%): ^{1}H NMR ($CDCl_3$, 400 MHz) δ 7.68 (s, 2H), 5.23 (s, 2H), 4.24 (q, J = 7.1 Hz, 2H), 1.27 (t, J = 7.1 Hz, 3H); CIMS m/z 156 (M+1).

5.1.10.2. Step 2: Ethyl 3-(4-bromophenyl)-2-(1*H*-1,2,3-triazol-1-yl)propanoate (15h). Prepared from ester **14h** (2.0 g, 12.89 mmol) following general method IV. Purification by column chromatography afforded bromide **15h** as a pale yellow oil (1.21 g, 29%): ^{1}H NMR ($CDCl_3$, 400 MHz) δ 7.67 (d, J = 1.0 Hz, 1H), 7.63 (d, J = 1.0 Hz, 1H), 7.35 (d, J = 8.5 Hz, 2H), 6.89 (d, J = 8.5 Hz, 2H), 5.54 (dd, J = 8.7, 6.5 Hz, 1H), 4.21 (q, J = 7.1 Hz, 2H), 3.47 (dd, J = 14.1, 6.3 Hz, 1H), 3.42 (dd, J = 14.1, 8.5 Hz, 1H), 1.22 (t, J = 7.3 Hz, 3H); CIMS m/z 324 $(M)^+$.

5.1.10.3. Step 3: 3-{4-[3-(5-Methyl-2-phenyl-oxazol-4-yl)-propyl]-phenyl}-2-1,2,3-triazol-1-yl-propionic acid ethyl ester (16h). Prepared from bromide **15h** (1.2 g, 3.702 mmol) using the general method II. Ester **16h** was obtained as a thick oil (1.00 g, 61%): ^{1}H NMR ($CDCl_3$, 400 MHz) δ 7.99–7.97 (m, 2H), 7.66 (d, J = 1.0 Hz, 1H), 7.63 (d, J = 1.0 Hz, 1H), 7.44–7.38 (m, 3H), 7.06 (d, J = 8.0 Hz, 2H), 6.93 (d, J = 8.0 Hz, 2H), 5.59 (dd, J = 8.3, 6.6 Hz, 1H), 4.19 (q, J = 7.3 Hz, 2H), 3.47 (dd, J = 14.1, 6.6 Hz, 1H), 3.41 (dd, J = 14.1, 8.5 Hz, 1H), 2.61 (t, J = 7.6 Hz, 2H), 2.48 (t, J = 7.3 Hz, 2H), 2.27 (s, 3H), 1.96 (qn, J = 7.8 Hz, 2H), 1.21 (t, J = 7.1 Hz, 3H); CIMS m/z 445 (M+1).

5.1.10.4. Step 4: 3-{4-[3-(5-Methyl-2-phenyl-oxazol-4-yl)-propyl]-phenyl}-2-1,2,3-triazol-1-yl-propionic acid (17h). Prepared from ester **16h** (1.0 g, 2.249 mmol) following the general method III. Acid **17h** was obtained as white solid (0.854 g, 91%): mp 162–163.5 °C; ^{1}H NMR ($CDCl_3$, 400 MHz) δ 7.94–7.92 (m, 2H), 7.66 (s, 1H), 7.63 (s, 1H), 7.42–7.40 (m, 3H), 7.01 (d, J = 8.0 Hz, 2H), 6.92 (d, J = 8.0 Hz, 2H), 5.62 (dd, J = 8.3, 6.1 Hz, 1H), 3.43 (dd, J = 14.4, 6.1 Hz, 1H), 3.38 (dd, J = 14.1, 8.3 Hz, 1H), 2.56 (t, J = 7.3 Hz, 2H), 2.48 (t, J = 7.3 Hz, 2H), 2.28 (s, 3H), 1.89 (qn, J = 7.8 Hz, 2H); CIMS m/z 417 (M+1). Anal. Calcd for $C_{24}H_{24}N_4O_3$·0.26 formic acid: C, 68.01; H, 5.77; N, 13.08. Found: C, 68.31; H, 5.88; N, 12.69.

5.1.11. 3-{4-[3-(5-Methyl-2-phenyl-oxazol-4-yl)-propyl]-phenyl}-2-1,2,3-triazol-2-yl-propionic acid (17i)

5.1.11.1. Step 1: Ethyl 3-(4-bromophenyl)-2-(2*H*-1,2,3-triazol-2-yl)propanoate (15i). Ester **14i** (3.0 g, 19.336 mmol) was dissolved in dry THF (60 mL) and cooled to −78 °C under a nitrogen atmosphere. A 1.0 M solution of potassium *tert*-butoxide in THF (20.3 mL, 20.3 mmol) was added. The mixture was stirred at −78 °C for 45 min. A solution of 4-bromobenzyl bromide (5.56 g, 22.236 mmol) in THF (20 mL) was added. The reaction was allowed to reach room temperature slowly and then stirred for 6 days. The mixture was quenched with water (60 mL) and diluted with diethyl ether and ethyl acetate. The phases were separated and the aqueous phase was extracted with diethyl ether-ethyl acetate (10:1, 55 mL × 3). The combined organic extracts were washed with brine, dried over magnesium sulfate and the solvent removed. Purification by column chromatography on silica gel eluting with ethyl acetate in hexanes (0–16%) afforded bromide **15i** as an oil (1.668 g, 26%): ^{1}H NMR ($CDCl_3$, 400 MHz) δ 7.62 (s, 2H), 7.32 (d, J = 8.5 Hz, 2H), 6.97 (d, J = 8.5 Hz, 2H), 5.48 (dd, J = 10.4, 5.4 Hz, 1H), 4.19 (q, J = 7.1 Hz, 2H), 3.67 (dd, J = 14.4, 10.5 Hz, 1H), 3.57 (dd, J = 14.4, 5.1 Hz, 1H), 1.54 (s, 3H), 1.20 (t, J = 7.1 Hz, 3H); CIMS m/z 324 $(M)^+$; Anal. Calcd for $C_{13}H_{14}BrN_3O_2$: C, 48.17; H, 4.35; N, 12.96. Found: C, 48.22; H, 4.06; N, 12.81.

5.1.11.2. Step 2: 3-{4-[3-(5-Methyl-2-phenyl-oxazol-4-yl)-propyl]-phenyl}-2-1,2,3-triazol-2-yl-propionic acid ethyl ester (16i). Prepared from bromide **15i** (2.148 g, 6.626 mmol), following general method II. Purification by column chromatography afforded ester **16i** as a thick oil (2.37 g, 80%): ^{1}H NMR ($CDCl_3$, 400 MHz) δ 7.98–7.95 (m, 2H), 7.61 (s, 2H), 7.44–7.38 (m, 3H), 7.03 (d, J = 8.3 Hz, 2H), 7.00 (d, J = 8.3 Hz, 2H), 5.50 (dd, J = 10.2, 5.6 Hz, 1H), 4.18 (q, J = 7.1 Hz, 2H), 3.67 (dd, J = 14.4, 10.1 Hz, 1H), 3.58 (dd, J = 14.1, 5.4 Hz, 1H), 2.58 (t, J = 7.6 Hz, 2H), 2.46 (t, J = 7.6 Hz, 2H), 2.24 (s, 3H), 1.93 (qn, J = 7.6 Hz, 2H), 1.19 (t, J = 7.1 Hz, 3H); CIMS m/z 445 (M+1).

5.1.11.3. Step 3: 3-{4-[3-(5-Methyl-2-phenyl-oxazol-4-yl)-propyl]-phenyl}-2-1,2,3-triazol-2-yl-propionic acid (17i). Prepared from ester **16i** (2.37 g, 5.331 mmol) following general method III. Acid **17i** was obtained as an off-white solid (2.11 g, 95%): mp 153–153.5 °C; ^{1}H NMR ($CDCl_3$, 400 MHz) δ 7.98–7.96 (m, 2H), 7.62 (s, 2H), 7.43–7.40 (m, 3H), 7.03 (d, J = 8.1 Hz, 2H), 6.98 (d, J = 8.1 Hz, 2H), 5.52 (dd, J = 10.4, 5.0 Hz, 1H), 3.62 (dd, J = 14.4, 10.2 Hz, 1H), 3.52 (dd, J = 14.4, 5.1 Hz, 1H), 2.58 (t, J = 7.6 Hz, 2H), 2.48 (t, J = 7.6 Hz, 2H), 2.27 (s, 3H), 1.93 (qn, J = 7.6 Hz, 2H); CIMS m/z 417 (M+1); Anal. Calcd for $C_{24}H_{24}N_4O_3$·0.1H_2O: C, 68.92; H, 5.83; N, 13.39. Found: C, 68.68; H, 5.75; N, 13.29.

5.1.12. (*S*)-3-{4-[3-(5-Methyl-2-phenyl-oxazol-4-yl)-propyl]-phenyl}-2-1,2,3-triazol-2-yl-propionic acid (17j)

The enantiomers of acid **17i** (7.06 g) were separated by preparative chiral HPLC: chiralpak AD column, 4.6 × 250 mm; mobile phase A: 70% hexanes with 0.1% TFA; mobile phase B: 30% ethanol; flow rate: 1 mL/min; detection at 285 nm. Compound **17j** was obtained as a solid (3.24 g): mp 125 °C; $[\alpha]_D^{25} = -89.8$ (c 0.53, THF); ^{1}H NMR and MS were identical to racemate. Enantiomer purity: 100%, retention time = 6.06 min. Anal. Calcd for $C_{24}H_{24}N_4O_3$·0.04H_2O: C, 69.09; H, 5.82; N, 13.43. Found: C, 68.70; H, 5.87; N, 13.38.

5.1.13. (*R*)-3-{4-[3-(5-Methyl-2-phenyl-oxazol-4-yl)-propyl]-phenyl}-2-1,2,3-triazol-2-yl-propionic acid (17k)

From the same purification, acid **17k** was obtained as a solid (0.797 g): $[\alpha]_D^{25} = +85.9$ (c 0.54, THF); ^{1}H NMR and MS were identical to racemate. Enantiomer purity: 99.06%, retention time = 9.44 min. Anal. Calcd for $C_{24}H_{24}N_4O_3$: C, 69.21; H, 5.81; N, 13.45. Found: C, 68.86; H, 5.87; N, 13.30.

5.2. General biology

The PPARα scintillation proximity assay was carried out as reported elsewhere.[44] All other PPAR in vitro assays and the *ob*/*ob* mouse study were carried out as previously reported.[19]

5.2.1. In vivo ZDF rat studies

Male Zucker Diabetic Fatty (ZDF/Crl-*Lepr*^{fa}) rats were obtained from Charles River Laboratories (Wilmington, MA).[39] The ZDF male rat normally presents with NIDDM, transient hyperinsulinemia and hypertriglyceridemia. Rats were pair housed under a 12-h light/dark cycle with free access to water and Purina 5008 rat chow (Protein 26.8%, fat 16.7%, carbohydrates 56.5% kcal/vol; Purina Mills, Richmond, IN). Prior to the onset of diabetic hyperglycemia (approximately 6 weeks of age, fed blood glucose <200 mg/dL), rats were allocated into groups by following a post-prandial, conscious tail venipuncture. Tail venipuncture in non-anesthetized, post-prandial animals was performed weekly to determine blood glucose, insulin, triglycerides, cholesterol and free fatty acid measurements. Insulin was determined by ELISA (Alpco, Inc.) and lipids determined enzymatically (Wako, Richmond) on a Cobas Mira Analyzer (Roche). Rats were administered a once daily oral dose for 2 weeks with suspensions of vehicle alone (1.5% carboxymethylcellulose, 0.2% Tween-20), or vehicle plus test compound at the specified dose. All experiments utilizing animals were reviewed

and approved by Pfizer's Institutional Animal Care and Use Committee.

5.2.2. Human ApoA1/CETP mouse model

Human ApoA1/CETP mice were bred at the Pfizer colony maintained at Charles River Laboratories (Wilmington, MA). Eight week old male mice were individually housed in solid bottom caging under a 12-h light/dark cycle with free access to water and standard Purina 5001 rodent chow (Purina Mills, Richmond, IN). Mice were administered a once daily oral dose for 14 days with suspensions of vehicle alone (1.5% carboxymethyl-cellulose, 0.2% Tween-20), or vehicle plus **17j** at 0.3, 1, 3, or 10 mg/kg/day compound. A terminal cardiac puncture post CO_2 inhalation provided blood sample for ApoA1, triglycerides, cholesterol and cholesterol fraction measurements. Lipids were determined by Cobas Mira Analyzer (Roche) and cholesterol fractions were separated by FPLC.[45] All experiments utilizing animals were reviewed and approved by Pfizer's Institutional Animal Care and Use Committee.

5.3. Pharmacokinetic studies

The study in rat was performed as previously described.[19]

5.3.1. Pharmacokinetic studies in dog

A study was conducted to determine the single dose pharmacokinetics and absolute oral bioavailability of **17j** following intravenous and oral administration to male beagle dogs. In a crossover design, dogs (n = 3/group) were administered a single 3 mg/kg capsule or a 1 mg/kg intravenous dose as a 5 min infusion. The intravenous dose was administered as a solution in 5% DMA/95% Tris Base (50 mM) (v:v), and the oral dose was administered, in a capsule, as a suspension in 5% PEG200/95% Methylcellulose (0.5% in sterile water) (v:v). Serial blood samples (for plasma) were collected from each dog over a 24-h period after dosing. Plasma concentrations of **17j** were determined using a validated achiral LC/MS/MS method. Pharmacokinetic parameters of **17j** were determined from the plasma concentration–time data using noncompartmental methods.

5.4. X-ray crystallography

A truncated construct of human PPARγ ligand binding domain (PPARγ-LBD) containing residues Glu207 to Tyr477 was recombinantly expressed in *E. coli* and purified as previously described.[20] A 12 mg/mL solution of apo human PPARγ-LBD was crystallized at 13 °C using the hanging drop vapor diffusion method over a 0.6 mL well solution consisting of 0.6–0.8 M tri-sodium citrate, 0.1 M imidazole pH 8 and 1 mM TCEP. Crystals were soaked overnight in a 0.8 mM solution of **17j** at room temperature prior to flash-cooling in 25% glycerol. X-ray diffraction data were collected at a wavelength of 1.00 Å at 100 K on the Industrial Macromolecular Crystallographer Association (IMCA) beam-line 17-ID at the Advanced Photon Source, Argonne National Labs. Diffraction data were processed using Denzo and Scalepack in the HKL2000 program suite.[46] The space group was determined to be centered monoclinic C2 with two molecules per asymmetric unit, corresponding to a solvent content of 52.2%.[47] The structure was determined by the method of molecular replacement using a monomer of human PPARγ-LBD (1I7I) with the ligand and waters removed as a search model with the program MOLREP in the CCP4i suite.[48–51] Structural refinement calculations and electron density maps were calculated with the program REFMAC5 in the CCP4i suite using the complete data with no resolution or sigma cutoff.[51,52] Manual fitting and real space refinement of the model was performed with the program QUANTA-2000 (Accelrys Inc., San Diego, CA). The final model of PPARγ-LBD consists of two monomers of PPARγ-LBD, 2 molecules of **17j** and 113 water molecules with the refinement statistics, R_{work} = 24.1%, R_{free} = 29.7% (see Supplementary data). The coordinates and structure factors may be found in the Protein Data Bank under the ID codes: 3IA6.pdb and 3IA6.sf.

5.5. Electrostatic potential calculations

The electrostatic potential maps were generated using Jaguar (version 7.5, Schrödinger, LLC, New York, NY, 2008). All structures were optimized using the B3LYP functional and 6-31G** basis set. The electrostatic potential and electron density surface were also calculated along with the optimization. The electrostatic potentials were superimposed on a constant electron density (0.002 e/a.u.^{3}) to mimic the Van de Waals surface of the molecule. The red represents negative electrostatic potential, and the blue indicates positive electrostatic potential.

Acknowledgements

Use of the IMCA-CAT beamline 17-ID at the Advanced Photon Source was supported by the companies of the Industrial Macromolecular Crystallography Association through a contract with Illinois Institute of Technology. Use of the Advanced Photon Source was supported by the US Department of Energy, Office of Science, Office of Basic Energy Sciences, under Contract No. W-31-109-Eng-38.

Supplementary data

Supplementary data associated with this article can be found, in the online version, at doi:10.1016/j.bmc.2009.09.001.

References and notes

1. Willson, T. M.; Brown, P. J.; Sternbach, D. D.; Henke, B. R. *J. Med. Chem.* **2000**, *43*, 527.
2. Berger, J.; Moller, D. E. *Annu. Rev. Med.* **2002**, *53*, 409.
3. Li, A. C.; Palinski, W. *Annu. Rev. Pharmacol. Toxicol.* **2006**, *46*, 1.
4. Guerre-Millo, M.; Gervois, P.; Raspe, E.; Madsen, L.; Poulain, P.; Derudas, B.; Herbert, J.; Winegar, D. A.; Wilson, T. M.; Fruchart, J.; Berge, R. K.; Staels, B. *J. Biol. Chem.* **2000**, *275*, 16638.
5. Ye, J.; Doyle, P.; Iglesias, M.; Watson, D.; Cooney, G.; Kraegen, E. *Diabetes* **2001**, *50*, 411.
6. Kobayashi, M.; Shigeta, Y.; Hirata, Y.; Omori, Y.; Sakamoto, N.; Nambu, S.; Baba, S. *Diabetes Care* **1988**, *11*, 495.
7. (a) Lehmann, J. M.; Moore, L. B.; Smith Oliver, T. A.; Wilkison, W. O.; Willson, T. M.; Kliewer, S. A. *J. Biol. Chem.* **1995**, *270*, 12953; (b) Wilson, T. M.; Cobb, J. E.; Cowan, D. J.; Wiethe, R. W.; Correa, I. D.; Prakash, S. R.; Beck, K. D.; Moore, L. B.; Kliewer, S. A.; Lehmann, J. M. *J. Med. Chem.* **1996**, *39*, 665.
8. (a) Nesto, R. W.; Bell, D.; Bonow, R. O.; Fonseca, V.; Grundy, S. M.; Horton, E. S.; Le Winter, M.; Porte, D.; Semenkovich, C. F.; Smith, S.; Young, L. H.; Kahn, R. *Diabetes Care* **2004**, *27*, 256; (b) Yki-Järvinen, H. *N. Eng. J. Med.* **2004**, *351*, 1106.
9. (a) Henke, B. R. *J. Med. Chem.* **2004**, *47*, 4118; (b) Fiévet, C.; Fruchart, J.-C.; Staels, B. *Curr. Opin. Pharm.* **2006**, *6*, 606.
10. Savkur, R. S.; Miller, A. R. *Exp. Opin. Invest. Drugs* **2006**, *15*, 763.
11. Ramachandran, U.; Kumar, R.; Mittal, A. *Mini-Rev. Med. Chem.* **2006**, *6*, 563.
12. Cheng, P. T. W.; Mukherjee, R. *Mini-Rev. Med. Chem.* **2005**, *5*, 741.
13. Henke, B. R.; Blanchard, S. G.; Brackeen, M. F.; Brown, K. K.; Cobb, J. E.; Collins, J. L., ; Harrington, W. W., Jr.; Hashim, M. A.; Hull-Ryde, E. A.; Kaldor, I.; Kliewer, S. A.; Lake, D. H.; Leesnitzer, L. M.; Lehmann, J. M.; Lenhard, J. M.; Orband-Miller, L. A.; Miller, J. F.; Mook, R. A.; Noble, S. A.; Oliver, W.; Parks, D. J.; Plunket, K. D.; Szewczyk, J. R.; Willson, T. M. *J. Med. Chem.* **1998**, *41*, 5020.
14. Lohray, B. B.; Lohray, V. B.; Bajji, A. C.; Kalchar, S.; Poondra, R. R.; Padakanti, S.; Chakrabarti, R.; Vikramadithyan, R. K.; Misra, P.; Juluri, S.; Mamidi, N. V. S. R.; Rajagopalan, R. *J. Med. Chem.* **2001**, *44*, 2675.
15. Ljung, B.; Bamberg, K.; Dahllof, B.; Kjellstedt, A.; Oakes Nicholas, D.; Ostling, J.; Svensson, L.; Camejo, G. *J. Lipid Res.* **2002**, *43*, 1855.
16. Murakami, K.; Tobe, K.; Ide, T.; Mochizuki, T.; Ohashi, M.; Akanuma, Y.; Yazaki, Y.; Kadowaki, T. *Diabetes* **1998**, *47*, 1841.
17. Devasthale, P. V.; Chen, S.; Jeon, Y.; Qu, F.; Shao, C.; Wang, W.; Zhang, H.; Farrelly, D.; Golla, R.; Grover, G.; Harrity, T.; Ma, Z.; Moore, L.; Ren, J.; Seethala, R.; Cheng, L.; Sleph, P.; Sun, W.; Tieman, A.; Wetterau, J. R.; Doweyko, A.; Chandrasena, G.; Chang, S. Y.; Humphreys, W. G.; Sasseville, V. G.; Biller, S. A.; Ryono, D. E.; Selan, F.; Hariharan, N.; Cheng, P. T. W. *J. Med. Chem.* **2005**, *48*, 2248.

18. Grundy, S. M. *Nat. Rev. Drug Disc.* **2006**, *5*, 295.
19. Casimiro-Garcia, A.; Bigge, C. F.; Davis, J. A.; Padalino, T.; Pulaski, J.; Ohren, J. F.; McConnell, P.; Kane, C. D.; Royer, L. J.; Stevens, K. A.; Auerbach, B.; Collard, W.; McGregor, C.; Fakhoury, S.; Schaum, R. P.; Zhou, H. *Bioorg. Med. Chem.* **2008**, *16*, 4883.
20. Nolte, R. T.; Wisely, G. B.; Westin, S.; Cobb, J. E.; Lambert, M. H.; Kurokawa, R.; Rosenfeld, M. G.; Willson, T. M.; Glass, C. K.; Milburn, M. V. *Nature* **1998**, *395*, 137.
21. Miyaura, N.; Ishiyama, T.; Ishikawa, M.; Suzuki, A. *Tetrahedron Lett.* **1986**, *27*, 6369.
22. Chemler, S. R.; Trauner, D.; Danishefsky, S. J. *Angew. Chem., Int. Ed.* **2001**, *40*, 4544.
23. Hoye, T. R.; Duff, S. R.; King, R. S. *Tetrahedron Lett.* **1985**, *26*, 3433.
24. Ohba, M.; Kawase, N.; Fujii, T. *J. Am. Chem. Soc.* **1996**, *118*, 8250.
25. Parks, D. J.; Tomkinson, N. C. O.; Villeneuve, M. S.; Blanchard, S. G.; Willson, T. M. *Bioorg. Med. Chem. Lett.* **1998**, *8*, 3657.
26. Takamura, M.; Sakurai, M.; Yamada, E.; Fujita, S.; Yachi, M.; Takagi, T.; Isobe, A.; Hagisawa, Y.; Fujiwara, T.; Yanagisawa, H. *Bioorg. Med. Chem.* **2004**, *12*, 2419.
27. Liu, K. G.; Lambert, M. H.; Ayscue, A. H.; Henke, B. R.; Leesnitzer, L. M.; Oliver, W. R., Jr.; Plunket, K. D.; Xu, H. E.; Sternbach, D. D.; Willson, T. M. *Bioorg. Med. Chem. Lett.* **2001**, *11*, 3111.
28. Keller, H.; Devchand, P. R.; Perroud, M.; Wahli, W. *Biol. Chem.* **1997**, *378*, 651.
29. Brown, P. J.; Winegar, D. A.; Plunket, K. D.; Moore, L. B.; Lewis, M. C.; Wilson, J. G.; Sundseth, S. S.; Koble, C. S.; Wu, Z.; Chapman, J. M.; Lehmann, J. M.; Kliewer, S. A.; Willson, T. M. *J. Med. Chem.* **1999**, *42*, 3785.
30. Xu, Y.; Rito, C. J.; Etgen, G. J.; Ardecky, R. J.; Bean, J. S.; Bensch, W. R.; Bosley, J. R.; Broderick, C. L.; Brooks, D. A.; Dominianni, S. J.; Hahn, P. J.; Liu, S.; Mais, D. E.; Montrose-Rafizadeh, C.; Ogilvie, K. M.; Oldham, B. A.; Peters, M.; Rungta, D. K.; Shuker, A. J.; Stephenson, G. A.; Tripp, A. E.; Wilson, S. B.; Winneroski, L. L.; Zink, R.; Kauffman, R. F.; McCarthy, J. R. *J. Med. Chem.* **2004**, *47*, 2422.
31. Wang, M.; Winneroski, L. L.; Ardecky, R. J.; Babine, R. E.; Brooks, D. A.; Etgen, G. J.; Hutchison, D. R.; Kauffman, R. F.; Kunkel, A.; Mais, D. E.; Montrose-Rafizadeh, C.; Ogilvie, K. M.; Oldham, B. A.; Peters, M. K.; Rito, C. J.; Rungta, D. K.; Tripp, A. E.; Wilson, S. B.; Xu, Y.; Zink, R. W.; McCarthy, J. R. *Bioorg. Med. Chem. Lett.* **2004**, *14*, 6113.
32. Nomura, M.; Tanase, T.; Ide, T.; Tsunoda, M.; Suzuki, M.; Uchiki, H.; Murakami, K.; Miyachi, H. *J. Med. Chem.* **2003**, *46*, 3581.
33. Miyachi, H.; Uchiki, H. *Bioorg. Med. Chem. Lett.* **2003**, *13*, 3145.
34. Uchiki, H.; Miyachi, H. *Chem. Pharm. Bull.* **2004**, *52*, 365.
35. Xu, H. E.; Lambert, M. H.; Montana, V. G.; Plunket, K. D.; Moore, L. B.; Collins, J. L.; Oplinger, J. A.; Kliewer, S. A.; Gampe, R. T., Jr.; McKee, D. D.; Moore, J. T.; Willson, T. M. *Proc. Natl. Acad. Sci. U.S.A.* **2001**, *98*, 13919.
36. Street, I. P.; Armstrong, C. R.; Withers, S. G. *Biochemistry* **1986**, *25*, 6021.
37. Davis, A. M.; Teague, S. J. *Angew. Chem., Int. Ed.* **1999**, *38*, 736.
38. Ross, S. A.; Gulve, E. A.; Wang, M. *Chem. Rev.* **2004**, *104*, 1255.
39. Clark, J. B.; Palmer, C. J.; Shaw, W. N. *Proc. Soc. Exp. Biol. Med.* **1983**, *173*, 68.
40. Yang, B.; Clifton, L. G.; McNulty, J. A.; Chen, L.; Brown, K. K.; Baer, P. G. *J. Cardiovasc. Pharmacol.* **2003**, *42*, 436.
41. (a) Chaput, E.; Saladin, R.; Silvestre, M.; Edgar, A. D. *Biochem. Biophys. Res. Commun.* **2000**, *271*, 445; (b) Carmona, M. C.; Louche, K.; Nibbelink, M.; Prunet, B.; Bross, A.; Desbazeille, M.; Dacquet, C.; Renard, P.; Casteilla, L.; Penicaud, L. *Int. J. Obes.* **2005**, *29*, 864.
42. (a) Fu, J.; Gaetani, S.; Oveisi, F.; Lo Verme, J.; Serrano, A.; Rodriguez de Fonseca, F.; Rosengarth, A.; Luecke, H.; Di Giacomo, B.; Tarzia, G.; Piomelli, D. *Nature* **2003**, *425*, 90; (b) Cano, C.; Pavon, J.; Serrano, A.; Goya, P.; Paez, J. A.; Rodriguez de Fonseca, F.; Macias-Gonzalez, M. *J. Med. Chem.* **2007**, *50*, 389; (c) O'Sullivan, S. E. *Br. J. Pharmacol.* **2007**, *152*, 576.
43. Kume, M.; Kubota, T.; Kimura, Y.; Nakashimizu, H.; Motokawa, K.; Nakano, M. *J. Antibiot.* **1993**, *46*, 177.
44. Guo, Q.; Sahoo, S. P.; Wang, P.-R.; Milot, D. P.; Ippolito, M. C.; Wu, M. S.; Baffic, J.; Biswas, C.; Hernandez, M.; Lam, M.-H.; Sharma, N.; Han, W.; Kelly, L. J.; Macnaul, K. L.; Zhou, G.; Desai, R.; Heck, J. V.; Doebber, T. W.; Berger, J. P.; Moller, D. E.; Sparrow, C. P.; Chao, Y.-S.; Wright, S. D. *Endocrinology* **2004**, *145*, 1640.
45. Kieft, K. A.; Bocan, T. M.; Krause, B. R. *J. Lipid Res.* **1991**, *32*, 859.
46. Otwinowski, Z.; Minor, W.. In Carter, C. W., Jr., Sweet, R. M., Eds.; Macromolecular Crystallography, Part A; Academic Press: New York, 1997; Vol. 276, pp 307–326.
47. Matthews, B. W. *J. Mol. Biol.* **1974**, *82*, 513.
48. Cronet, P.; Petersen, J. F. W.; Folmer, R.; Blomberg, N.; Sjoblom, K.; Karlsson, U.; Lindstedt, E.-L.; Bamberg, K. *Structure* **2001**, *9*, 699.
49. Berman, H. M.; Battistuz, T.; Bhat, T. N.; Bluhm, W. F.; Bourne, P. E.; Burkhardt, K.; Feng, Z.; Gilliland, G. L.; Iype, L.; Jain, S.; Fagan, P.; Marvin, J.; Padilla, D.; Ravichandran, V.; Schneider, B.; Thanki, N.; Weissig, H.; Westbrook, J. D.; Zardecki, C. *Acta Crystallogr., Sect. D* **2002**, *58*, 899.
50. Vagin, A. A.; Teplyakov, A. *J. Appl. Crystallogr.* **1997**, *30*, 1022.
51. Collaborative Computational Project No. 4. *Acta Crystallogr., Sect. D.* **1994** *50*, 760–763.
52. Murshudov, G. N.; Vagin, A. A.; Dodson, E. J. *Acta Crystallogr., Sect. D* **1997**, *53*, 240.